Geoscientific
Model Development

Development and technical paper

GEO4PALM v1.1: an open-source geospatial data processing toolkit for the PALM model system

Dongqi Lin[1], **Jiawei Zhang**[2], **Basit Khan**[3,a], **Marwan Katurji**[1], **and Laura E. Revell**[4]

[1]Te Kura Aronukurangi, School of Earth and Environment, University of Canterbury, Ōtautahi / Christchurch, New Zealand
[2]Scion, New Zealand Forest Research Institute Limited, Ōtautahi / Christchurch, New Zealand
[3]Geoinformatics for Climate Resilient Urban Systems (GRUSS), Institute of Photogrammetry and Remote Sensing (IPF), Karlsruhe Institute of Technology (KIT), 76131 Karlsruhe, Germany
[4]Te Kura Matū, School of Physical and Chemical Sciences, University of Canterbury, Ōtautahi / Christchurch, New Zealand
[a]now at: Mubadala Arabian Center for Climate and Environmental Sciences (ACCESS), New York University Abu Dhabi, Abu Dhabi, United Arab Emirates

Correspondence: Dongqi Lin (dongqi.lin@canterbury.ac.nz)

Abstract. A geospatial data processing tool, GEO4PALM, has been developed to generate geospatial static input for the Parallelized Large-Eddy Simulation (PALM) model system. PALM is a community-driven large-eddy simulation model for atmospheric and environmental research. Throughout PALM's 20-year development, research interests have been increasing in its application to realistic conditions, especially for urban areas. For such applications, geospatial static input is essential. Although abundant geospatial data are accessible worldwide, geospatial data availability and quality are highly variable and inconsistent. Currently, the geospatial static input generation tools in the PALM community heavily rely on users for data acquisition and pre-processing. New PALM users face large obstacles, including significant time commitments, to gain the knowledge needed to be able to pre-process geospatial data for PALM. Expertise beyond atmospheric and environmental research is frequently needed to understand the data sets required by PALM. Here, we present GEO4PALM, which is a free and open-source tool. GEO4PALM helps users generate PALM static input files with a simple, homogenised, and standardised process. GEO4PALM is compatible with geospatial data obtained from any source, provided that the data sets comply with standard geo-information formats. Users can either provide existing geospatial data sets or use the embedded data interfaces to download geo-information data from free online sources for any global geographic area of interest. All online data sets incorporated in GEO4PALM are globally available, with several data sets having the finest resolution of 1 m. In addition, GEO4PALM provides a graphical user interface (GUI) for PALM domain configuration and visualisation. Two application examples demonstrate successful PALM simulations driven by geospatial input generated by GEO4PALM using different geospatial data sources for Berlin, Germany, and Ōtautahi / Christchurch, New Zealand. GEO4PALM provides an easy and efficient way for PALM users to configure and conduct PALM simulations for applications and investigations such as urban heat island effects, air pollution dispersion, renewable energy resourcing, and weather-related hazard forecasting. The wide applicability of GEO4PALM makes PALM more accessible to a wider user base in the scientific community.

1 Introduction

The Parallelized Large-Eddy Simulation (PALM) model is a large-eddy simulation (LES) model that has been used for atmospheric boundary layer (ABL) research for over 20 years (Maronga et al., 2015, 2020; Raasch and Schröter, 2001). PALM is a free and open-source model with high scalability to simulate atmospheric flows from the mesoscale (10 to 200 km) to the microscale (1 cm to 1 km). To resolve land surface physics, PALM provides several features including

the radiative transfer model (RTM; Krč et al., 2021), land surface model (LSM; Gehrke et al., 2021), urban surface model (USM; Resler et al., 2017), and plant canopy model (PCM; Maronga et al., 2020). Over the last few years, PALM has been extensively developed for various microscale and mesoscale applications, especially for wind energy and urban applications. With the implementation of new modules, PALM has been used to study wind turbine wake in a German wind farm (Vollmer et al., 2017) and urban environments, such as ventilation in the city of Hong Kong (Gronemeier et al., 2017) and urban air quality and pollutant dispersion in Cambridge, the United Kingdom (Kurppa et al., 2019); Helsinki, Finland (Kurppa et al., 2020); and Bergen, Norway (Wolf et al., 2020, 2021). In addition, several studies (e.g. Belda et al., 2021; Resler et al., 2021; Salim et al., 2022) have carried out sensitivity analysis and simulations to validate PALM in urban environments. Geospatial data sets that describe the land surface characteristics and provide ground surface boundary conditions to the atmospheric model are critical for realistic simulations, especially for microscale and/or urban climate studies.

The exchanges of energy and moisture between the surface and the atmosphere are impacted by physical characteristics of the land surface, such as urban canopy, plant canopy, topography, and land use, across a spectrum of spatial and temporal scales throughout the atmospheric boundary layer (ABL; e.g. Bou-Zeid et al., 2004; Maronga et al., 2014; Rihani et al., 2015; Srivastava et al., 2020). To include, resolve, and realise the near-surface physical characteristics, PALM's current initialisation setup allows users to provide a NetCDF static driver strictly formatted in PALM Input Data Standard (PIDS) as an input (hereafter referred to as the static driver). In PALM, geospatial data should be processed and stored in a static driver to carry out simulations. Heldens et al. (2020) described the data requirements of the static driver for PALM and provided the PALM Create Static Driver tool (hereafter PALM CSD) to generate a static driver for PALM using geospatial data. However, the data processing routine provided by Heldens et al. (2020) is heavily dependent on the geospatial data set prepared by the German Space Agency (DLR), for example, for three cities in Germany (Stuttgart, Berlin, and Hamburg) described in their study. The PALM CSD tool can only process data in NetCDF format with its particular data standard, which requires users to dedicate significant time to pre-processing the geospatial data.

In addition to PALM CSD, palmpy (https://github.com/stefanfluck/palmpy, last access: 29 January 2024; Fluck, 2020) is another tool developed to generate static driver input for PALM applications at the Centre for Aviation (ZAV), Zurich University of Applied Sciences, Switzerland (Liu et al., 2022). The palmpy tool is more generally applicable compared to PALM CSD, but, to the best of our knowledge, it has mainly been applied to regions in Switzerland. Another tool for PALM static drivers is the PALM-4U GUI developed at the Fraunhofer Institute for Building Physics (https: //gitlab.cc-asp.fraunhofer.de/palm_gui/palm4u_gui; last access: 7 November 2023). This tool, however, was only recently made public, and its user manual is still under construction at the time of writing. Users are responsible for a significant amount of data pre-processing before using these tools. Therefore, in many other regions, for instance, New Zealand, where only a small number of geospatial data sets have been prepared by local authorities, big hurdles still exist to apply PALM with realistic land surface characteristics. Numerous geospatial data sets can be used to generate the PALM static driver, while the spatial coverage, resolution, data quality, and data format could vary. PALM simulations for urban applications may require high-resolution geospatial input, but PALM can also be used for applications of a coarse resolution over a large area. Users are required to search and identify the appropriate geospatial data sets for their PALM applications. In addition, the final conversion to PALM-readable formats requires extra processing. These issues go beyond the understanding and knowledge of physical processes and may have prevented further applications of PALM in the community. Furthermore, the lack of a highly applicable static driver preparation tool likely hinders the reproducibility of scientific results across different regions and research groups.

Looking at the history of numerical weather prediction (NWP) models, the Weather Research and Forecasting (WRF) model is arguably one of the most popular numerical atmospheric models in the world, and its broader development has been community-driven (Powers et al., 2017). The community effort has empowered WRF users towards more advanced research and operational applications. In the WRF community, tools and packages have been developed with community contributions (e.g. as cited in Meyer and Riechert, 2019, and Powers et al., 2017, and references therein). In contrast, the supporting tools for the PALM community are still limited. As discussed in Maronga et al. (2020), more development of PALM is still needed to broaden its applicability and accessibility and to strengthen its position within the boundary layer and urban climate scientific community. Through developing accessible and user-friendly tools with continuous efforts from the community, PALM has the opportunity to become as popular and widely used as WRF.

We have developed a widely applicable geo-information toolkit containing a set of routines written in the Python programming language designed to process geospatial data for PALM simulations. This tool is hereafter referred to as GEO4PALM. GEO4PALM can interface with several free online application programming interfaces (APIs), allowing users to obtain domain-specific information from globally available databases. For users who have obtained their geospatial data from other sources, GEO4PALM can process any geospatial data in GeoTIFF format regardless of the data source. With GEO4PALM, users can include land surface characteristics such as topography, land use, and build-

ing and plant canopy information in their PALM simulations. Here, we describe and document the GEO4PALM toolkit. The PALM static driver features covered by GEO4PALM are described in Sect. 2. Along with the framework and workflow of GEO4PALM, Sect. 3 presents detailed descriptions and requirements of the input data and the online data interfaces for GEO4PALM. Two application examples of GEO4PALM are given in Sect. 4. Conclusions, discussions on the limitations, and an outlook of GEO4PALM are presented in Sect. 5.

2 PALM features in GEO4PALM

The hierarchy and data format of the variables in the static driver of PALM are described in PIDS (https://palm.muk.uni-hannover.de/trac/wiki/doc/app/iofiles/pids, last access: 20 June 2023) and by Heldens et al. (2020). Depending on the application, PALM simulations can include surface features such as buildings, pavements, and plants. In GEO4PALM, two settings are available for users to choose from. One is the default or the minimum setting, and the other allows users to add additional features for the urban surface and plant canopies. For the minimum setting, the static driver is incorporated with all the required variables to conduct a PALM simulation, while all the additional features are optional. Although GEO4PALM does not cover all the available features presented in PIDS, it includes most of the available features, including basic urban features such as buildings, pavements, and streets, which are sufficient to represent most urban and plant canopies. The variables covered by GEO4PALM are presented in Table 1.

3 GEO4PALM framework

An early version of GEO4PALM was applied in simulations presented by Lin et al. (2021, 2023). However, this version (GEO4PALM v1.0) was only applicable for geospatial data for Ōtautahi / Christchurch, New Zealand. In this paper, several new features have been added to GEO4PALM v1.1. The new design of GEO4PALM v1.1 aims to (1) allow users to create static drivers for PALM simulations regardless of the geospatial data sources and (2) simplify the workflow of generating the static driver. The file steering structure of GEO4PALM is shown in Fig. 1. The main source code of GEO4PALM is stored in the `util` folder with the main executable Python script (`run_config_static.py`) located in the main directory. The `JOBS` folder allows users to create static driver files for multiple jobs (x, y, z, etc.). In each job directory, users must have an `INPUT` folder, which includes a configuration file, a land use type lookup table, and all input geospatial data files for the static driver. The `TMP` folder stores all temporary files, and all static driver files are created and stored in the `OUTPUT` folder.

The framework of GEO4PALM is shown in Fig. 2. Users must at least provide a configuration file, which

contains PALM domain configuration details and the data sources of static driver input. GEO4PALM uses Python packages including Xarray, Rasterio, rioxarray, GeoPandas, and geocube (Hoyer and Hamman, 2017; Gillies et al., 2019; Jordahl et al., 2020; Snow et al., 2022a, b) to process the geo-information data. When converting geospatial data into the static driver, GEO4PALM requires input files in GeoTIFF format, while no requirement is set regarding the spatial resolution and projection of the GeoTIFF files. The geospatial input data are resampled automatically based on the grid spacing values specified in the configuration file. Users have the freedom to choose the resampling method depending on their simulation needs. For details of the available options, users are referred to the Rasterio documentation (https://rasterio.readthedocs.io/en/stable/api/rasterio.enums.html#rasterio.enums.Resampling; last access: 23 June 2023). In addition to the GeoTIFF format, the shapefile format is one of the most common file types for geospatial data. Differently from the rasterised GeoTIFF files, the shapefiles are usually vectorised with multiple layers, and each layer has its own designated name, which varies with the data set. Due to the complexity of shapefiles, it is exhaustive to include shapefiles and all the embedded layers as a direct input in GEO4PALM. Therefore, a script `shp2tif.py` is provided as a GEO4PALM pre-processing tool for users to convert shapefiles to GeoTIFF format of the desired resolution (the finest in the input configuration file by default). This script converts one layer of the shapefile at a time, allowing users to choose the layer based on their applications. Table 2 explains all variables contained in the configuration file. A step-by-step guide for GEO4PALM and a sample configuration file are provided in Appendix A.

In the configuration file, users need to specify the desired geographic projection, domain configuration, and geospatial input data source for PALM simulations. If the desired projection of PALM simulations is not specified, GEO4PALM will use the nearest Universal Transverse Mercator (UTM) projection based on the latitude and longitude of the PALM domain centre given in the configuration file. To visualise PALM domain locations and to help users build the domain configuration easily, GEO4PALM is incorporated with a web-based interactive graphical user interface (GUI; Fig. 3). The GUI is generated by the `palm_domain_utility.py` script. This PALM domain utility allows users to render grid boxes of PALM domains over satellite and aerial imagery obtained from Environmental Systems Research Institute (Esri) World Imagery (https://geoviews.org/gallery/bokeh/tile_sources.html; last access: 19 June 2023) through open-source Python libraries including Panel and GeoViews (https://panel.holoviz.org/ and https://geoviews.org/; last access: 19 June 2023). The utility automatically checks and adjusts the domain configuration to avoid violations of rules for PALM domain nesting such as overlapping of domain boundaries and mismatching of the grid between parent and child domains. More de-

Table 1. List of variables GEO4PALM can include in the PALM static driver. For more detailed descriptions of the variables, refer to Heldens et al. (2020) and PIDS (https://palm.muk.uni-hannover.de/trac/wiki/doc/app/iofiles/pids, last access: 20 June 2023).

Variable name	Feature	Description
zt	Required	Terrain height above sea level in metres
vegetation_type	Required	Classification of vegetation types at the land surface
pavement_type	Required	Classification of pavement types at the land surface
water_type	Required	Classification of waterbodies
soil_type	Required	Classification of soil types, usually specified for corresponding vegetation types
surface_fraction	Required	Relative fraction of the respective surface type given – depending on vegetation_type, pavement_type, and water_type
albedo_type	Optional	Optional classification of albedo for land surface
water_pars	Optional	Optional parameters for waterbodies, including water temperature, roughness length for momentum, emissivity, etc.
lad	Optional	Three-dimensional leaf area density in $m^2 m^{-3}$; required for the plant canopy model to resolve vegetation canopy
street_type	Optional	Optional classification of street type; required for application of the parameterised traffic emissions and the multi-agent system
building_type	Optional	Classification of building types; required for buildings in the urban surface model
buildings_2d	Optional	Heights of buildings relative to the underlying terrain; required for buildings in the urban surface model
building_id	Optional	Building ID to identify individual building envelopes; required for buildings in the urban surface model
buildings_3d	Optional	Three-dimensional building topology relative to the underlying terrain; required for buildings in the urban surface model

tails for using the PALM domain GUI are described in the GEO4PALM user manual (https://github.com/dongqi-DQ/GEO4PALM; last access: 7 November 2023).

Users are not required to have a full set of input data. For each geospatial input field, users can provide their own data in GeoTIFF or shapefile format and download data from online sources when some of the data sets are not locally available. For geospatial files provided by users, one needs to specify the file name in the configuration file. If one desires to use online data, the data source should be specified. For the time being, we provide several interfaces to download data sets with global coverage. Water temperature, the digital elevation model (DEM), and land use are the three mandatory elements to create a static driver. Water temperature is an important factor which can have an impact on boundary layer structure (e.g. Mahrt and Hristov, 2017), while by default PALM prescribes a water temperature of 283.0 K for all waterbodies. Therefore, water temperature is required in GEO4PALM. Users can provide their own water temperature map in a GeoTIFF file or a prescribed wa-

ter temperature in the configuration file for all waterbodies in the simulation domains. Alternatively, users can use the online sea surface temperature (SST) data set downloaded by GEO4PALM. As SST is widely available across various global data sets, we provide an interface to download SST data to represent water temperature for waterbodies in the GEO4PALM static driver. The SST data (resolution of 0.01°) are obtained using the Earthdata Common Metadata Repository (CMR) API operated by the National Aeronautics and Space Administration (NASA), which is linked to the OPeN-DAP interface (Open-source Project for a Network Data Access Protocol; https://lpdaac.usgs.gov/tools/opendap/; last access: 20 May 2023). The NASA data sets are available globally, and users are required to register an account to use the data freely. By default, GEO4PALM downloads version 4.1 of the Multi-scale Ultra-high Resolution (MUR) of the Group for High Resolution Sea Surface Temperature (GHRSST) Level-4 analysis provided by NASA's Jet Propulsion Laboratory (NASA/JPL, 2015; Chin et al., 2017). The water temperature is obtained from the grid point of the SST
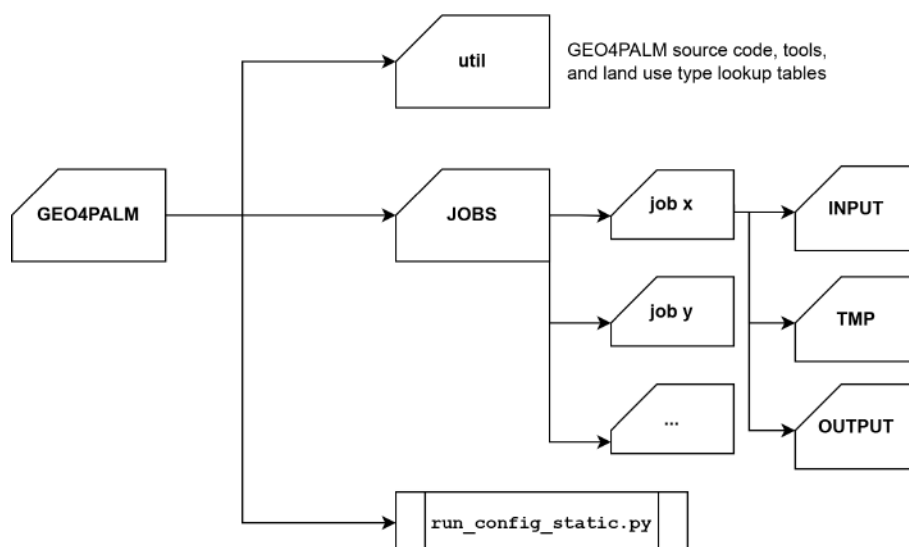
Figure 1. GEO4PALM file steering outline. The main executable script is `run_config_static.py`. The `util` folder contains all GEO4PALM utilities, including the source code, tools, and land use classification lookup table. Within the `JOBS` folder, each user-specified job is stored separately with input files in `INPUT`, temporary files in `TMP`, and output files in `OUTPUT`.

data set nearest to the PALM simulation domains. To download and use this data set, users must specify `online` in the configuration file for the variable `water`. The date and time of the SST data should be specified using the parameter `origin_time` in the `[case]` section. If users have spatial water temperature data available for waterbodies in GeoTIFF format, they can specify the data file name in the configuration file for the variable `water`. Users are also allowed to prescribe a fixed water temperature for each simulation domain using the `water_temperature` parameter in the `[settings]` section.

The DEM (spatial resolution of 30 m) and land use classification are available to download from the Application for Extracting and Exploring Analysis Ready Samples (A$\rho\rho$EEARS; https://appeears.earthdatacloud.nasa.gov/; last access: 7 November 2023) operated by NASA. The DEM is the product of NASA Shuttle Radar Topography Mission 1 arcsec NetCDF V003 (SRTMGL1_NC.003) acquired by spaceborne radar (Rabus et al., 2003). For the NASA data, users may provide the start and end date for the data acquisition such that the land use is representative of the simulation period. GEO4PALM source code provides a lookup table (Table B1) for the MODIS Land Cover Type product (A$\rho\rho$EEARS product code: LC_type1), which converts the land use classification to PALM-recognisable values. The MODIS Land Cover Type product supplies global land cover maps at 500 m spatial resolution dated from 2001 (Friedl and Sulla-Menashe, 2019). More options for land use classification data sources provided by NASA refer to A$\rho\rho$EEARS online documentation (https://appeears.earthdatacloud.nasa.gov/; last access: 7 November 2023). If users desire to download and use A$\rho\rho$EEARS data sets, they must specify `nasa` in the configuration file for the variables `dem` and/or `lu`.

In addition to the A$\rho\rho$EEARS interface, GEO4PALM incorporates the application programming interface that connects to the worldwide land cover mapping data products (WorldCover; https://esa-worldcover.org/en; last access 7 November 2023) operated by the European Space Agency (ESA). The ESA WorldCover data have a spatial resolution of 10 m (Zanaga et al., 2021, 2022). Users must register a free account to obtain data from ESA. A lookup table (Table B2) for PALM-readable conversion is provided in the GEO4PALM source code. For the usage of ESA data, users are required to specify `esa` in the configuration file for the variable `lu`. In addition to the lookup tables for NASA and ESA data, the GEO4PALM source code provides a lookup table (Table B3) for the New Zealand Land Cover Database (LCDB) V5.0 (Landcare Research, 2020). All the lookup tables are presented in Appendix B.

All urban and plant fields can be left blank ("") in cases where users do not require such features in the static driver. If users desire to have other land surface features, GEO4PALM can process data for the urban surface model and plant canopy model. In PALM, urban surfaces include pavements, buildings, and streets. Although according to PIDS v1.12, the typology of streets is represented by the variable `pavement_type` and the variable `street_type` is only used for the chemistry model in PALM, GEO4PALM still includes the variable `street_type` such that the static driver can be used for simulations that require the chemistry model and/or the multi-agent system. Like the DEM and land use data, users can either provide their own GeoTIFF data or choose to download data online. If users wish to pro-
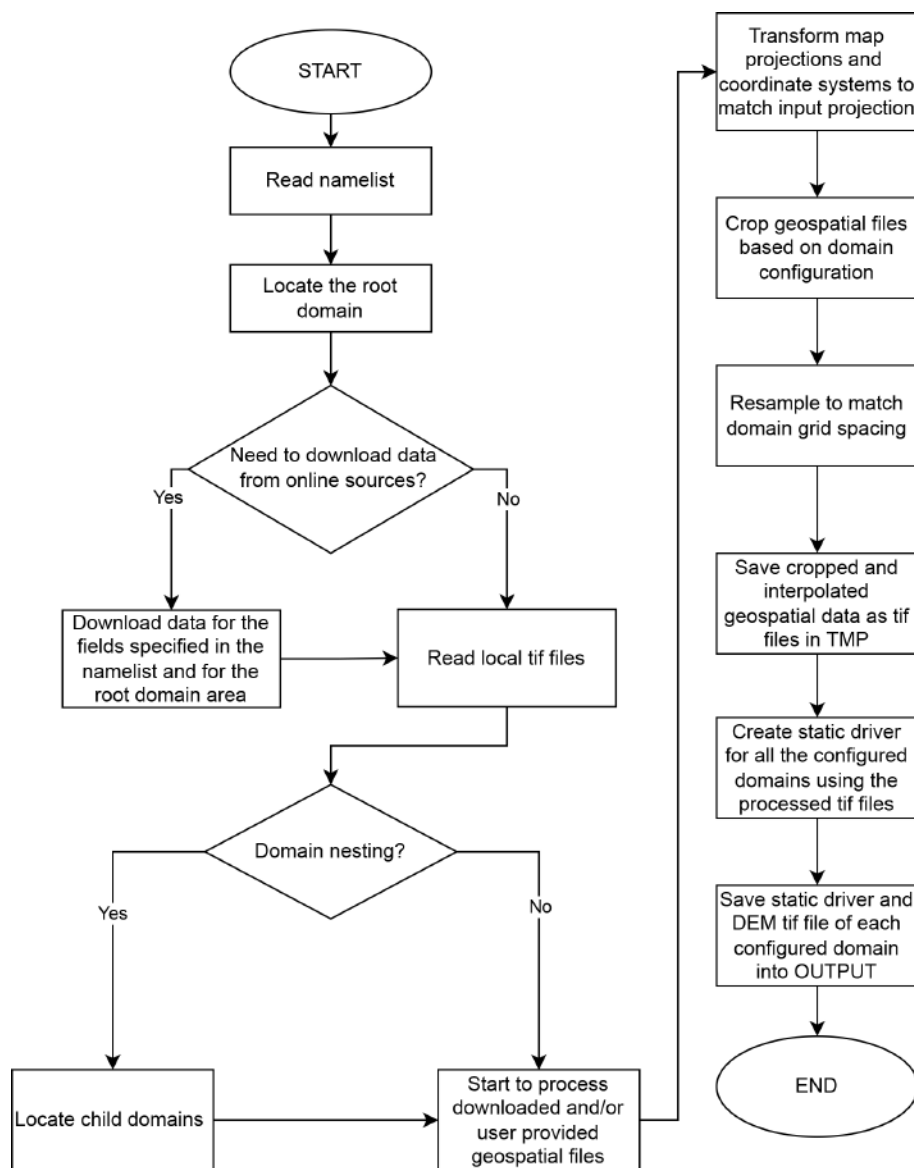
Figure 2. Flowchart showing the code structure of GEO4PALM.

vide their own data, they must provide GeoTIFF files with building height at the building location, building ID for each building, PALM-recognisable pavement types for each pavement, and/or PALM-recognisable street types for each street, separately. Otherwise, users can specify `osm` for the urban variables in the configuration file to download data from OpenStreetMap (OSM; https://www.openstreetmap.org/; last access: 7 November 2023). GEO4PALM uses the OSMnx package (Boeing, 2017) to obtain data from OSM. Downloaded OSM data sets are converted to PALM-recognisable data by GEO4PALM using the conversion described by Heldens et al. (2020). Note that OSM also provides land use classification but does not have a good spatial coverage for many regions in the world. Therefore, GEO4PALM currently

does not support OSM land cover data. Users are encouraged to use the OSM land cover data set with a modified land use type conversion table like those shown in Appendix B if their PALM simulations are conducted for regions with good spatial coverage of OSM land cover data. GEO4PALM is adaptable to any land use data provided in shapefile or GeoTIFF format.

For plant canopy, GEO4PALM currently only supports leaf area density (LAD; Lalic and Mihailovic, 2004) calculations based on vegetation height provided in the GeoTIFF files. To avoid noise from other surface geometry, GEO4PALM applies an automatic process in which surface objects with heights less than the filter (`tree_height_filter` in Table 2) are removed. With
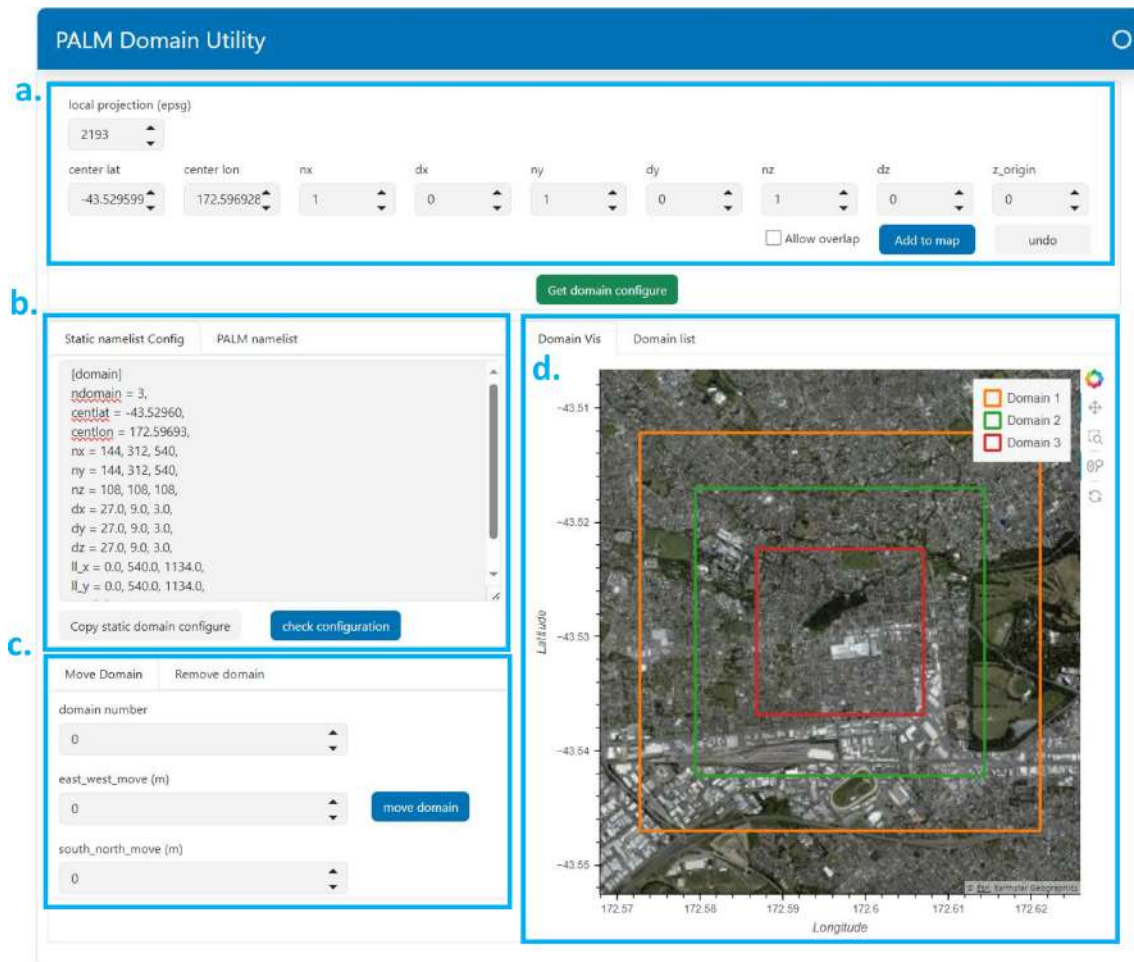
Figure 3. A screenshot of the web-based PALM domain utility GUI showing the domain configuration for the Ōtautahi / Christchurch case described in Sect. 4.3. Users can input domain configuration in the subtab **(a)**. The GUI automatically generates configuration parameters for both GEO4PALM and PALM domain configuration in the subtab **(b)**. Users can adjust the domain locations using the subtab **(c)**. PALM domains are drawn over the interactive satellite imagery in the subtab **(d)**.

this filter, objects like cars or fences are not included as vegetation. The default value of the filter is 1.5 m, and users can adjust the value in the configuration file. With high-quality data, this noise filter can be set to a desired low value (≥ 0.0 m) such that low objects, like grass, long grass, and bushes, can be included and represented in PALM simulations. The LAD calculation is adopted from PALM CSD (Heldens et al., 2020) and is based on the equation proposed by Lalic and Mihailovic (2004) as follows:

$$\mathrm{LAD}(z) = \mathrm{LAD_m} \left(\frac{h - z_\mathrm{m}}{h - z} \right)^n \exp\left[\left(1 - \frac{h - z_\mathrm{m}}{h - z} \right) n \right]$$
$$[\mathrm{m^2\,m^{-3}}], \qquad (1)$$

where $\mathrm{LAD_m}$ is the maximum LAD, h is the tree height, z_m is the height where LAD reaches $\mathrm{LAD_m}$, and $n = 6$ when $z < z_\mathrm{m}$ and $n = 0.5$ when $z \geq z_\mathrm{m}$. According to Kolic (1978) and Lalic and Mihailovic (2004), the normalised value of z_m

ranges from 0.2 to 0.4 depending on the tree type. Currently, GEO4PALM only allows users to provide a fixed value of leaf area index (LAI; `tree_lai_max` in Table 2) and z_m (`lad_max_height` in Table 2) values as input. LAI is recognised as the integration of LAD over the tree height (h). To derive LAD at each vertical level, GEO4PALM uses the given LAI and z_m with the integral form of Eq. (1) (refer to Lalic and Mihailovic, 2004, for more details). GEO4PALM automatically scales LAD based on the height of the vegetation canopy at individual grid points. This approach does not take account of spatial variation in LAD for different tree species, while it is still useful in cases where no LAD or LAI data are available. For cases in which LAD or LAI information is available, users are advised to adjust the code to directly read the spatial LAD/LAI information. However, to the best of our knowledge, no globally available vegetation height data, along with plant canopy data, are currently free to obtain from any online sources. Therefore, GEO4PALM

does not provide any online interface for this purpose. One possible solution to obtaining vegetation height is to calculate surface objects' height using the digital surface model (DSM) and DEM. In addition to the information on ground surface altitude contained in the DEM, the DSM supplies the heights of all surface objects, such as buildings and trees.

Once users have provided all required information in the configuration file along with their own geospatial data where applicable, GEO4PALM downloads and/or processes the input data to create the static driver. GEO4PALM allows users to configure nested domains and use different input data for each domain. To reduce the learning curve, the domain nesting configuration is similar to PALM's nesting module, in which the nested domain location is determined by the distance of the lower-left corners between the root domain and child domains. PALM's own input and output files can contain geospatial information, while the geospatial projection references sometimes may not be included accurately in a NetCDF file. Geospatial coordinates with correct geospatial projection could be important in real-world applications, especially when comparing PALM results to observations. To overcome this potential issue, instead of providing geospatial information in the NetCDF files, a GeoTIFF file with coordinate information is created by GEO4PALM along with each static driver. We recommend that GEO4PALM users use the GeoTIFF file to better reference the geospatial coordinate. For more details and examples, users are referred to the Supplement, which contains the input files for the case studies presented in Sect. 4.

4 Examples of real-world applications

4.1 Model and simulation configuration

As mentioned in Sect. 3, the aim of GEO4PALM is to allow users to use geospatial data for their PALM simulations seamlessly. Users may have data ready locally in GeoTIFF or shapefile format, or they can download all geospatial data freely for any location. Several other studies have used the input data described in this article and the earlier versions of GEO4PALM. For example, the static input generated by GEO4PALM was used for Christchurch Airport to demonstrate applications of the WRF4PALM offline nesting tool (Lin et al., 2021). Lin et al. (2023) have used GEO4PALM-generated static input for fog research over the city of Ōtautahi / Christchurch.

In this section, we present two examples, both using GEO4PALM and PALM CSD, to demonstrate the performance and compatibility of GEO4PALM. One example is Berlin, Germany (52.516615° N, 13.402782° E), and the other is Ōtautahi / Christchurch, New Zealand (43.529599° S, 172.596928° E). We have used the online API for both cases to obtain geospatial input. For Berlin, we have geospatial data sets prepared and stored locally containing to-

pography, streets, buildings, waterbodies, vegetation, etc., at 2 m resolution. These data have been processed by the German Space Agency (DLR) similarly to those described by Khan et al. (2021) and Heldens et al. (2020). Hereafter, we refer to the local data sets for Berlin as the DLR data sets. We have used the same DLR data sets to run both PALM CSD described by Heldens et al. (2020) and GEO4PALM with a map projection of EPSG:25833 (ETRS89/UTM zone 33N) to match the projection coded in PALM CSD. At present, PALM CSD only supports 10 UTM projections between zone 28N and zone 37N or a pre-processed rectangle map projection. Therefore, for Ōtautahi / Christchurch, we pre-processed all the local data to the map projection of EPSG:2193 (New Zealand Transverse Mercator) using geographic information system (GIS) software and the tools in GEO4PALM. Then, the corresponding GeoTIFF files were processed into PALM-CSD-compatible NetCDF files. Since PALM CSD does not provide land use classification conversion from other data sources, we first used GEO4PALM to convert our land use input data set to PALM-recognisable land use types. Then, we used GIS software with additional Python scripts to make our land use data sets compatible with PALM CSD.

Table 3 gives an overview of the simulations conducted for Berlin and Ōtautahi / Christchurch. Overall, we conducted six simulations, comprising three simulations for each of the two cities. The three simulations for Berlin are denoted Berlin_CSD, Berlin_GEO, and Berlin_OL, which used static drivers generated by PALM CSD, GEO4PALM with the DLR data sets, and GEO4PALM with online data sets, respectively. The three simulations for Ōtautahi / Christchurch are denoted Chch_CSD, Chch_GEO, and Chch_OL, which used static drivers generated by PALM CSD with local data sets, GEO4PALM with local data sets, and GEO4PALM with online data sets, respectively. For demonstration purposes, both examples have identical domain dimensions and grid spacing (shown in Table 4). All geospatial input data were resampled to match the grid spacing of the simulations. To demonstrate the LAD calculation in GEO4PALM, we used `tree_lai_max` = 5.0 and `lad_max_height` = 0.4, corresponding to pine trees, for both Berlin_GEO and Chch_GEO. The initialisation time was set to 00:00 UTC on 1 January 2021 for Ōtautahi / Christchurch and 12:00 UTC on 1 January for Berlin, which is midday summertime for Ōtautahi / Christchurch and around midday wintertime for Berlin. The simulation time is 6 h for both simulations. Due to the high computation cost with fine grid spacings, here we only performed simulations using domain nesting with the finest grid spacing at 3 m, while GEO4PALM can generate a static driver with grid spacings finer than 1 m, depending on the data source.

We used the PALM model system 22.10 to conduct the simulations. For demonstration purposes, all simulations were initialised with idealised forcing. A northerly was prescribed with a wind speed of $4 \, \mathrm{m \, s^{-1}}$. At the initialisation,

Table 2. Variables descriptions of the GEO4PALM input configuration file.

Variables	Descriptions	Comment
	Case	
case_name	Name of the case, identical to the job folder name.	
origin_time	Date and time to start the PALM simulation in "YYYY-MM-DD HH:mm:ss +HH" format. For example, 12:00 UTC on 21 June 2019 is "2019-06-21 12:00:00 +00".	Refer to origin_date_time in the PALM input configuration file for more details.
default_proj	The default projection (EPSG:4326) for GEO4PALM to use latitudes and longitudes to locate domains.	For most users, no changes are needed.
config_proj	The desired projection of the static driver.	A local projection with units in metres is recommended, for example, EPSG:2193 for New Zealand.
lu_table	File name of land use lookup table to convert land use classification to PALM-recognisable classifications.	Should be provided in the INPUT folder. Otherwise, GEO4PALM uses the default table provided in util.
	Settings	
water_temperature	User input water temperature values in kelvins when no water temperature data are available.	One value for each simulation domain.
building_height_dummy	User input dummy height in metres for buildings where building heights are missing in the online OpenStreetMap data set or if 0.0 m is provided as the building height in the input data.	One value for each simulation domain.
tree_height_filter	User input filter height in metres to remove small surface objects; i.e. if an object height is below this value, then this object is not included in the LAD estimation.	One value for each simulation domain.
	Domain	
ndomain	Maximum number of domains.	If ndomain ≥ 2, domain nesting is enabled.
centlat	Centre latitude of the root domain.	Not required for nested child domains.
centlon	Centre longitude of the root domain.	Not required for nested child domains.
nx	Number of grid points along the x axis.	The actual number of grid points along the x axis (nx). Note that this is different from the PALM configuration file (nx−1).
ny	Number of grid points along the y axis.	The actual number of grid points along the y axis (ny). Note that this is different from the PALM configuration file (ny−1).
nz	Number of grid points along the z axis.	
dx	Grid spacing in metres along the x axis.	
dy	Grid spacing in metres along the y axis.	
dz	Grid spacing in metres along the z axis.	
z_origin	Mean elevated terrain grid position in metres.	Default is 0.0 m.
ll_x	Lower-left corner distance to the first domain in metres along the x axis; only use when nesting is required.	
ll_y	Lower-left corner distance to the first domain in metres along the y axis; only use when nesting is required.	

Table 2. Continued.

Variables	Descriptions	Comment
	GeoTIFF	
water	Input data source for water temperature. Users need to specify the input file name, or data can be downloaded from OPeNDAP with the option `online`.	
dem	Input data source for topographical height. Users need to specify the file name, or data can be downloaded from NASA A$\rho\rho$RAS with the option `nasa`.	
lu	Input data source for land use classification. Users need to specify the file name, or data can be downloaded from NASA A$\rho\rho$RAS with the option `nasa` and/or from ESA WorldCover with the option `esa`.	A lookup table to convert land use typologies to PALM-recognisable values is required.
resample_method	Method to resample GeoTIFF files when interpolating/extrapolating to the desired grid spacing.	Default is `nearest`.
	If A$\rho\rho$RAS interface is used	
dem_start_date	DEM data start date in YYYY-MM-DD format.	Default is `2000-02-12` and no need to change if SRTMGL1_NC.003 data set is used.
dem_end_date	DEM data end date in YYYY-MM-DD format.	Default is `2000-02-20` and no need to change if SRTMGL1_NC.003 data set is used.
lu_start_date	Land use data start date in YYYY-MM-DD format.	Default is `2020-10-01` for product LC_Type01. Should be changed according to users' needs.
lu_end_date	Land use data end date in YYYY-MM-DD format.	Default is `2020-10-30` for product LC_Type01 Should be changed according to users' needs.
	Urban	
bldh	Input data source for building heights. Users need to specify the file name, or data can be downloaded from OSM with the option `online`.	
bldid	Input data source for the building ID. Users need to specify the file name, or data can be downloaded from OSM with the option `online`.	
pavement	Input data source for pavement types. Users need to specify the file name, or data can be downloaded from OSM with the option `online`.	
street	Input data source for street types. Users need to specify the file name, or data can be downloaded from OSM with the option `online`.	
	Plant	
tree_lai_max	Input value for maximum leaf area index.	
lad_max_height	Input value for z_m (range between 0.2 and 0.4) as described in Eq. (1).	
sfch	Input data source for plant height above the surface. Users need to specify the file name.	Currently, no online data source/interface is available.

the surface potential temperature is 295.65 K with no vertical gradient in the first 2000 m from the surface and a vertical gradient of 0.3 K per 100 m for the levels above 2000 m up to the top boundary. The prognostic equation for the water vapour mixing ratio is switched off. Periodic lateral boundary conditions are used with the clear-sky radiation scheme. The radiative transfer model (RTM; Krč et al., 2021) and land surface model (LSM; Gehrke et al., 2021) were switched on for all domains. The urban surface model (USM; Resler et al., 2017) and plant canopy model (PCM; Maronga et al., 2020) are only switched on for the child domains (N02 and N03).

4.2 Case study for Berlin

This section demonstrates a case study to compare the static drivers created by PALM CSD, GEO4PALM with local data, and GEO4PALM with online data. The input data sources used in GEO4PALM are listed in Table 5. For Berlin_CSD and Berlin_GEO, the data were processed by DLR. For details of the DLR data sets and PALM CSD, refer to Khan et al. (2021) and Heldens et al. (2020). As water temperature was not included in the DLR data set, we used GEO4PALM to obtain water temperature via the Earthdata API for Berlin_GEO. Regarding Berlin_OL, the only user input is the configuration file. GEO4PALM handled all data downloading from online sources, including the global GHRSST data, NASA 30 m DEM data (SRT-MGL1_NC.003), ESA WorldCover land use classification data, and OSM urban data sets.

The domain location and static driver data for Berlin_CSD, Berlin_GEO, and Berlin_OL are shown in Figs. 4 and 5. In Berlin_OL, several buildings are included in the simulation domain. However, the OSM data (used in the Berlin_OL simulation) do not contain building height for most buildings. Therefore, buildings with no height data available were assigned a height of 3.0 m for demonstration purposes. LAI, the vertically integrated LAD, shows areas with plant canopy in Fig. 4b and c. For the Berlin_OL case, LAD was not included in the static driver input, since we do not have any DEM or DSM with spatial resolution finer than 30 m. The LAI calculated by GEO4PALM (Fig. 4b) is higher than the one calculated by PALM CSD (Fig. 4c). In Berlin_GEO, the vegetation patch height data were directly used by GEO4PALM to estimate LAD, without considering vegetation type. In Berlin_CSD, however, vegetation type and the simulation season were considered. A lot of data processing is required to pre-process vegetation data for PALM CSD. For the estimation of LAD, at least the vegetation height, vegetation type, and LAI data are required. Considering the inconsistency in data sources and quality worldwide, GEO4PALM adopts the simplified method to calculate LAD. Both GEO4PALM and PALM CSD can be modified further by users depending on their modelling needs.

Berlin_GEO and Berlin_CSD present similar features in terrain heights (Fig. 4e and f) in which the shapes of rivers are distinguishable. However, the terrain heights in Berlin_OL (Fig. 4d) do not contain many details due to the coarse resolution of its data source. The online DEM data only have a spatial resolution of 30 m. Berlin_GEO and Berlin_CSD used the same geospatial input, and hence, the topography data for the two cases are identical. It should be noted that PALM CSD offers an option to modify the terrain height of the child domains to follow the average values of their corresponding parent domain, allowing for a smoother transition of the flow at the nested child domains' lateral boundaries. After this modification, PALM CSD can be configured to adjust the topography height onto the simulation domain's vertical levels. Currently, such adjustments are not included in GEO4PALM. GEO4PALM adopts the DEM directly and lets PALM itself process and convert topography into the simulation grid. These topography adjustment features are switched off for the comparison between PALM CSD and GEO4PALM presented here.

The vegetation type in Berlin_OL (Fig. 5a) also has a coarser resolution compared to Berlin_GEO (Fig. 5b) and Berlin_CSD (Fig. 5c) because the spatial resolution for the ESA land use data is 10 m. The difference in the vegetation-type classification between Berlin_OL and the other two simulations could be due to the conversion between the ESA WorldCover data set and PALM. Users are referred to Table B2 for the conversion, which can be edited depending on users' needs. Comparing Berlin_GEO (Fig. 5b) to Berlin_CSD (Fig. 5c), one can notice that vegetation patches classified as type 7 (deciduous broadleaf trees; brown patches in Fig. 5b) in Berlin_GEO are classified as type 3 (short grass; light purple in Fig. 5c) in Berlin CSD. This is caused by the adjustments applied in PALM CSD. It corrects vegetation type when a vegetation height is available and is indicative of low-lying plant cover. PALM CSD also alters the vegetation type for grid points where LAD data are available, i.e. where the plant canopies are resolved. This is to avoid numerical issues when using a high roughness length with small vertical grid spacing. In addition, a tall vegetation type with high roughness length plus the resolved plant canopies could over-represent the drag of the vegetation. Subsequently, the flow reduction may be overestimated. This feature is currently not available in GEO4PALM.

The pavement type and street type presented in Berlin_OL are generally similar to in Berlin_GEO and Berlin_CSD. As the widths of pavements and streets were generated automatically in Berlin_OL by GEO4PALM, some of the details, such as the width and type of each pavement and street, are of lower fidelity in Berlin_OL compared to those in Berlin_GEO and Berlin_CSD. This is similar regarding buildings. The structures and locations of buildings in Berlin_OL align with those in Berlin_GEO and Berlin_CSD. However, the DLR geospatial data do not include the Berlin Palace (as shown in the centre of Figs. 4a and 5j–l), while

Table 3. Overview of simulations for Berlin and Ōtautahi / Christchurch.

Simulation case name	Data source	Static driver generation tools
	Berlin	
Berlin_CSD	DLR data set (resolution of 2 m)	PALM CSD
Berlin_GEO	DLR data set (resolution of 2 m)	GEO4PALM
Berlin_OL	Online data sets included in GEO4PALM (refer to Table 5 for details)	GEO4PALM
	Ōtautahi / Christchurch	
Chch_CSD	Ōtautahi / Christchurch local data sets (refer to Table 6 for details)	PALM CSD
Chch_GEO	Ōtautahi / Christchurch local data sets (refer to Table 6 for details)	GEO4PALM
Chch_OL	Online data sets included in GEO4PALM (refer to Table 6 for details)	GEO4PALM

Table 4. Nested domain dimension summary. Here, x refers to the west–east coordinate, y refers to the south–north coordinate, and z refers to the vertical coordinate.

Domain	Number of grid points (x, y, z)	Domain size (x, y, z)	Horizontal grid spacing (dx, dy)	Vertical grid spacing (dz)
N01	$144 \times 144 \times 108$	$3888 \times 3888 \times 2916$	27 m	27 m
N02	$312 \times 312 \times 108$	$2808 \times 2808 \times 972$	9 m	9 m
N03	$540 \times 540 \times 108$	$1620 \times 1620 \times 324$	3 m	3 m

this building is present in Berlin_OL (Fig. 5j). This building was recently reconstructed and hence is not included in the DLR data set and subsequently not included in Berlin_GEO and Berlin_CSD.

Figures 6 and 7 illustrate the horizontal cross-sections of the simulation results. These results are hourly averages for the second and sixth (i.e last) hour of the simulations. The variables displayed include 2 m potential temperature (θ_{2m}), surface temperature (T_{sfc}), surface net radiation (R_{net}), and 10 m wind speed ($WS_{10 m}$) and direction. To compare the simulation results between GEO4PALM and PALM CSD, the differences between Berlin_OL and Berlin_CSD and between Berlin_GEO and Berlin_CSD are shown in Fig. 8. In all simulations, R_{net} and T_{sfc} are strongly dependent on the land surface type and surface canopy. Comparing Berlin_OL to Berlin_GEO, the differences show the impact of the geospatial data input. The topography input data for Berlin_OL have a resolution of 30 m. The coarse topography in Berlin_OL creates box-like features, especially for θ_{2m} (see Figs. 6a and 8a) and R_{net} (Fig. 7g) at the beginning of the simulation. Although Berlin_OL captures the building outlines in the simulation domain, the lack of accurate building height data leads to an underestimation of θ_{2m} (Fig. 8b) and an overestimation of $WS_{10 m}$ (Fig. 8j) compared to Berlin_CSD. In GEO4PALM, all buildings are configured as type 3 (residential buildings built after 2000) by default because we currently do not have a good local building-type data set to use as a reference. As a result of different building-type data sets, Berlin_OL shows an overestimation of T_{sfc} compared to Berlin_CSD (Fig. 8f). In addition, as the land use input data have a grid spacing of

10 m for Berlin_OL, the waterbodies were not presented with good fidelity in Berlin_OL, compared to Berlin_GEO and Berlin_CSD. This is reflected in the simulated R_{net} in Fig. 6j. As Berlin_OL uses a completely different geospatial data set compared to Berlin_CSD, the values of R_{net} in Berlin_OL for non-building areas are significantly higher than those in Berlin_CSD (Fig. 8m) in the second simulation hour. The differences are still considerable in the last simulation hour (Fig. 8n), suggesting the importance of the input data. The presence of the Berlin Palace in Berlin_OL shows a strong impact on the simulated temperature, wind, and net radiation. In more realistic applications, users should be careful about the geospatial data acquisition dates, especially in urban environments where building reconstructions frequently occur.

For a more direct comparison between GEO4PALM and PALM CSD, the results of Berlin_GEO and Berlin_CSD are presented. For the comparison in the second simulation hour, Berlin_GEO coincides with more variations in T_{sfc} and R_{net} than in θ_{2m} and $WS_{10 m}$ (Fig. 8). This is because T_{sfc} and R_{net} are more sensitive to the differences in the input water temperature, the input building types, adjustments applied in vegetation types, and LAD estimation methods. PALM CSD allows users to input the spatial distribution of water type and water temperature. Otherwise, it uses the default water temperature of 283.0 K embedded in the code. Similarly to PALM CSD, GEO4PALM allows a spatial input of water temperature. However, we do not have water temperature data available. For the Berlin case study, GEO4PALM obtained water temperature from the GHRSST data, which is 275.0 K. For comparison and demonstration purposes, we

Table 5. Geospatial input data for GEO4PALM used in the Berlin case study. Refer to Khan et al. (2021) and Heldens et al. (2020) for details of data sources for Berlin_CSD.

GEO4PALM variables	Data set	Source
Berlin_GEO		
water	GHRSST Level-4 MUR product	OPeNDAP via Earthdata (https://lpdaac.usgs.gov/tools/opendap/; last access: 7 November 2023)
dem	DLR data sets	Refer to Khan et al. (2021) and Heldens et al. (2020).
lu	DLR data sets	Refer to Khan et al. (2021) and Heldens et al. (2020).
bldh	DLR data sets	Refer to Khan et al. (2021) and Heldens et al. (2020).
bldid	DLR data sets	Refer to Khan et al. (2021) and Heldens et al. (2020).
pavement	DLR data sets	Refer to Khan et al. (2021) and Heldens et al. (2020).
street	DLR data sets	Refer to Khan et al. (2021) and Heldens et al. (2020).
sfch	DLR data sets	Refer to Khan et al. (2021) and Heldens et al. (2020).
Berlin_OL		
water	GHRSST Level-4 MUR product	OPeNDAP via Earthdata (https://lpdaac.usgs.gov/tools/opendap/; last access: 7 November 2023)
dem	NASA Shuttle Radar Topography Mission 1 arcsec NetCDF V003 (SRTMGL1_NC.003)	A$\rho\rho$EEARS (https://appeears.earthdatacloud.nasa.gov/; last access: 7 November 2023)
lu	ESA WorldCover 10 m (2020 V1)	TerraCatalogueClient (https://vitobelgium.github.io/terracatalogueclient; last access: 7 November 2023)
bldh	OSM	OpenStreetMap via OSMnx (Boeing, 2017)
bldid	OSM	OpenStreetMap via OSMnx (Boeing, 2017)
pavement	OSM	OpenStreetMap via OSMnx (Boeing, 2017)
street	OSM	OpenStreetMap via OSMnx (Boeing, 2017)
sfch	Not available	Not applicable

did not modify the default water temperature in PALM CSD, while users can modify the source code for their simulations. Such a difference in water temperature leads to significant contrasts in T_{sfc} (Fig. 8g–h) and R_{net} (Fig. 8o–p) between Berlin_GEO and Berlin_CSD. Over the river, θ_{2m} is also lower in Berlin_GEO. The same as Berlin_OL, only one building type is used in Berlin_GEO. This leads to higher T_{sfc} in Berlin_GEO later in the simulation (Fig. 8h). The differences in the building type also lead to a negative bias in the R_{net} differences for building areas in Berlin_GEO.

Adjustments in the vegetation type are evident in the surface variables (T_{sfc} and R_{net}; Fig. 8g–h and o–p), especially at the beginning of the simulations (Fig. 8g and o). Excluding the waterbodies and buildings, the blue patches in Fig. 8g coincide with the brown patches in the vegetation types of Berlin_GEO shown in Fig. 5b. Without the adjustments in the vegetation type, these vegetation patches in Berlin_GEO lead to a positive bias in R_{net} compared to Berlin_CSD

(Fig. 8o). In the last simulation hour, the cold biases in T_{sfc} in Berlin_GEO over the vegetation patches are less significant (Fig. 8h). Regarding R_{net}, the positive biases resemble the LAI patterns of Berlin_GEO shown in Fig. 4b, showing the potential impact of inaccurate LAD input. The signal of the adjusted vegetation type, however, is not clear in WS_{10m}, as shown in Fig. 8k–l. Without the vegetation-type adjustment, the wind speed is expected to be lower in Berlin_OL, while we cannot identify such an impact from Fig. 8k–l. More investigation is required to determine the appropriate adjustment in vegetation types.

Overall, the static driver generated by GEO4PALM and, subsequently, the simulation fidelity of PALM are highly dependent on the input geospatial data quality. With high-quality data, GEO4PALM can create static drivers (Berlin_GEO) that are comparable to PALM CSD (Berlin_CSD). Without local data, GEO4PALM can only represent the simulated environment with limited details, as
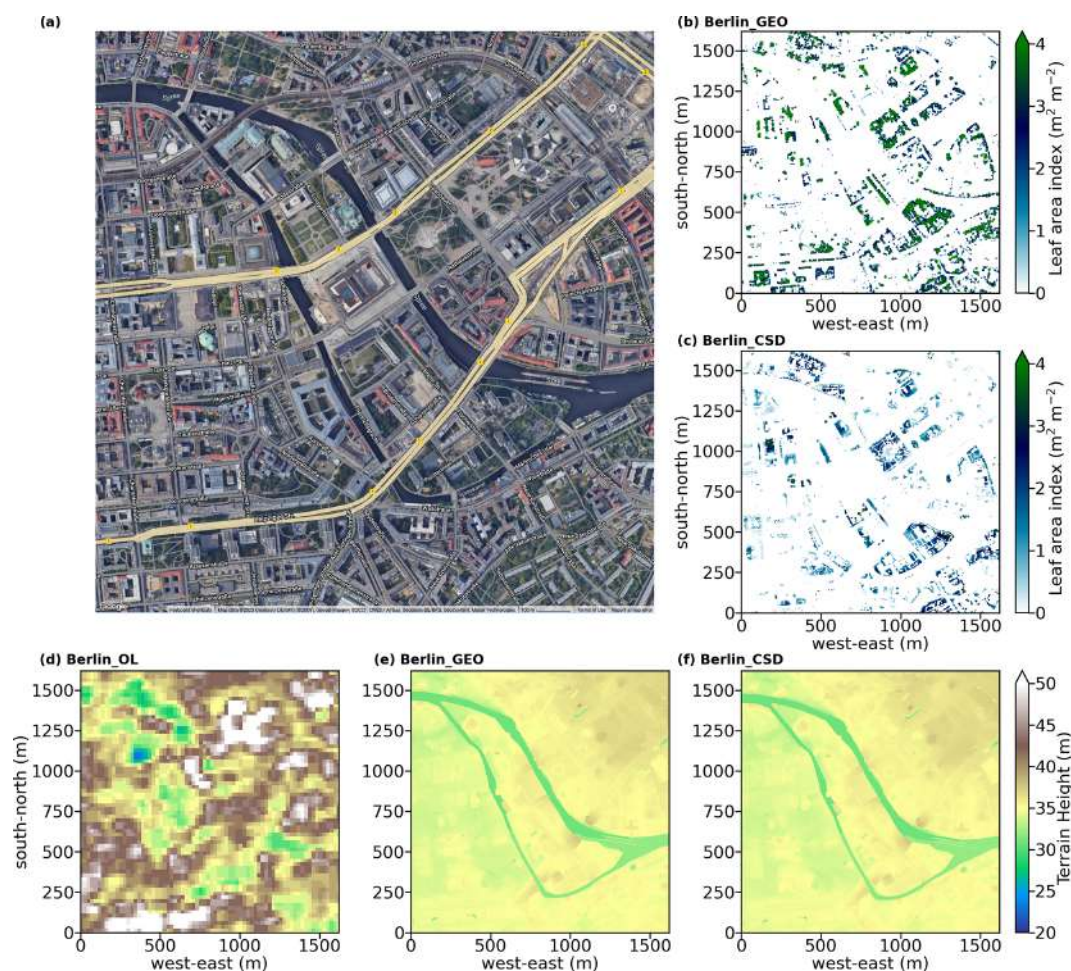
Figure 4. (a) Satellite images showing domain location of the nested domain N03 for the Berlin case (© Google Earth). Domain centre is located near the Humboldt Forum in central Berlin, Germany. The horizontal cross-sections of static input data: **(b–c)** LAI (vertically integrated LAD) and **(d–f)** terrain height. For data sources refer to Table 4. No LAI data are displayed for Berlin_OL, as no online data source is available for the estimation of LAD.

presented in Berlin_OL. The lack of building height information and the coarse resolution of the online data sets may not be suitable for a realistic simulation in the urban environment. These data sets, however, could be useful for coarse simulations, for example, the parent domains of the focused simulation area.

4.3 Case study for Ōtautahi / Christchurch

In this section, we present a case study for Ōtautahi / Christchurch, New Zealand, to demonstrate the application of GEO4PALM when the simulation location changes. Local geospatial data sets are used to demonstrate the suitability and applicability of GEO4PALM for the case Chch_GEO. Similarly to Berlin_OL, Chch_OL used all geospatial data downloaded by GEO4PALM rather than local data sets. PALM CSD was used for Ōtautahi / Christchurch using the same input as Chch_GEO, with the geospatial input files pre-processed into a specific NetCDF format.

The input data for this case study are listed in Table 6. The water temperature was obtained from the GHRSST data sets for both simulations. For Chch_GEO, the DEM was obtained from the Enviroinment Canterbury Regional Council (2020); the land use classification was obtained from New Zealand LCDB v5.0 (Landcare Research, 2020); the building footprint, location, and building ID were derived using OSM data and the NZ Building Outlines data set (Land Information New Zealand, 2020); the building height was calculated using the difference between the DSM and DEM at the building locations; the pavement and street data were obtained from OSM and converted to PALM-recognisable data using the conversion provided by Heldens et al. (2020); and the tree height was derived using the difference between the DSM and DEM with buildings excluded.

Figures 9 and 10 show the domain location and static input data for the nested domain of 3 m grid spacing (domain N03) for Chch_OL, Chch_GEO, and Chch_CSD. Riccarton
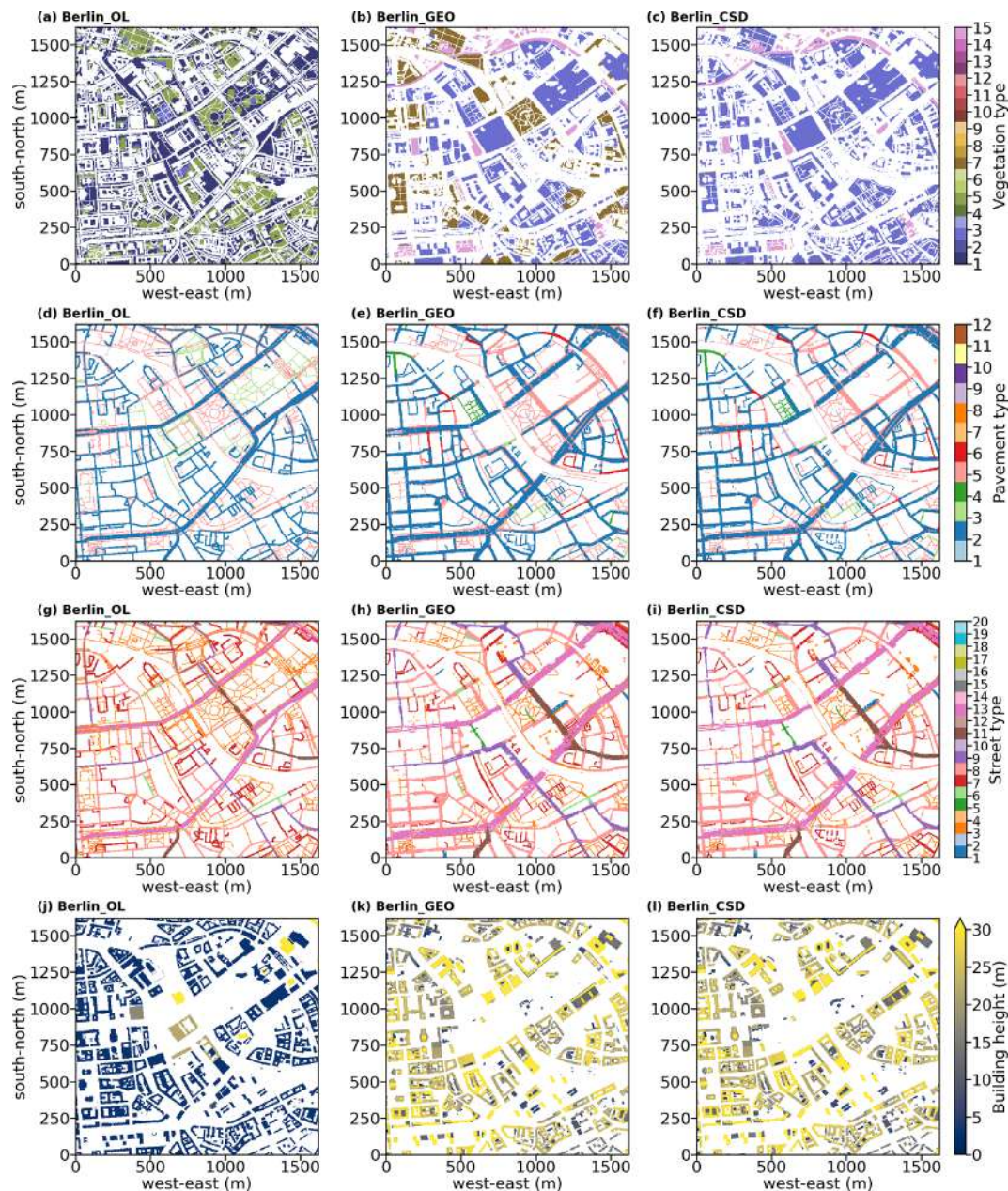
Figure 5. Static input data of the nested domain N03 for the Berlin case: **(a–c)** vegetation type, **(d–f)** pavement type, **(g–i)** street type, and **(j–l)** building height. Refer to the panel label for the corresponding simulation. For data sources refer to Table 5.

Bush is located near the centre of domain N03, with sports fields to its north and Westfield Riccarton (the largest building in the domain) to its south. Riccarton Bush coincides with high LAI over an area of approximately 98 000 m² , as shown in Fig. 9b. Again, due to the coarse resolution of the online DEM data, Chch_OL does not present good details of topography height (Fig. 9d) compared to Chch_GEO (Fig. 9e). However, Chch_OL does capture the decrease in topography from west to east of the domain. It should be noted that the NASA topography data may have included surface objects'

heights (compare Fig. 9d to Fig. 9e–f), while the DEM and topography in the concept of GEO4PALM and PALM refer to the topographical height only. Users should take extra care if they use the NASA topography data. As the New Zealand land use data set (New Zealand LCDB v5.0) classifies all urban area as only one type, most of the area within the city of Ōtautahi / Christchurch was identified as bare soil by GEO4PALM (Fig. 10b). This is different in the ESA World-Cover data set where Chch_OL shows more areas with vegetation type 5 (deciduous needleleaf trees; green in Fig. 10a),
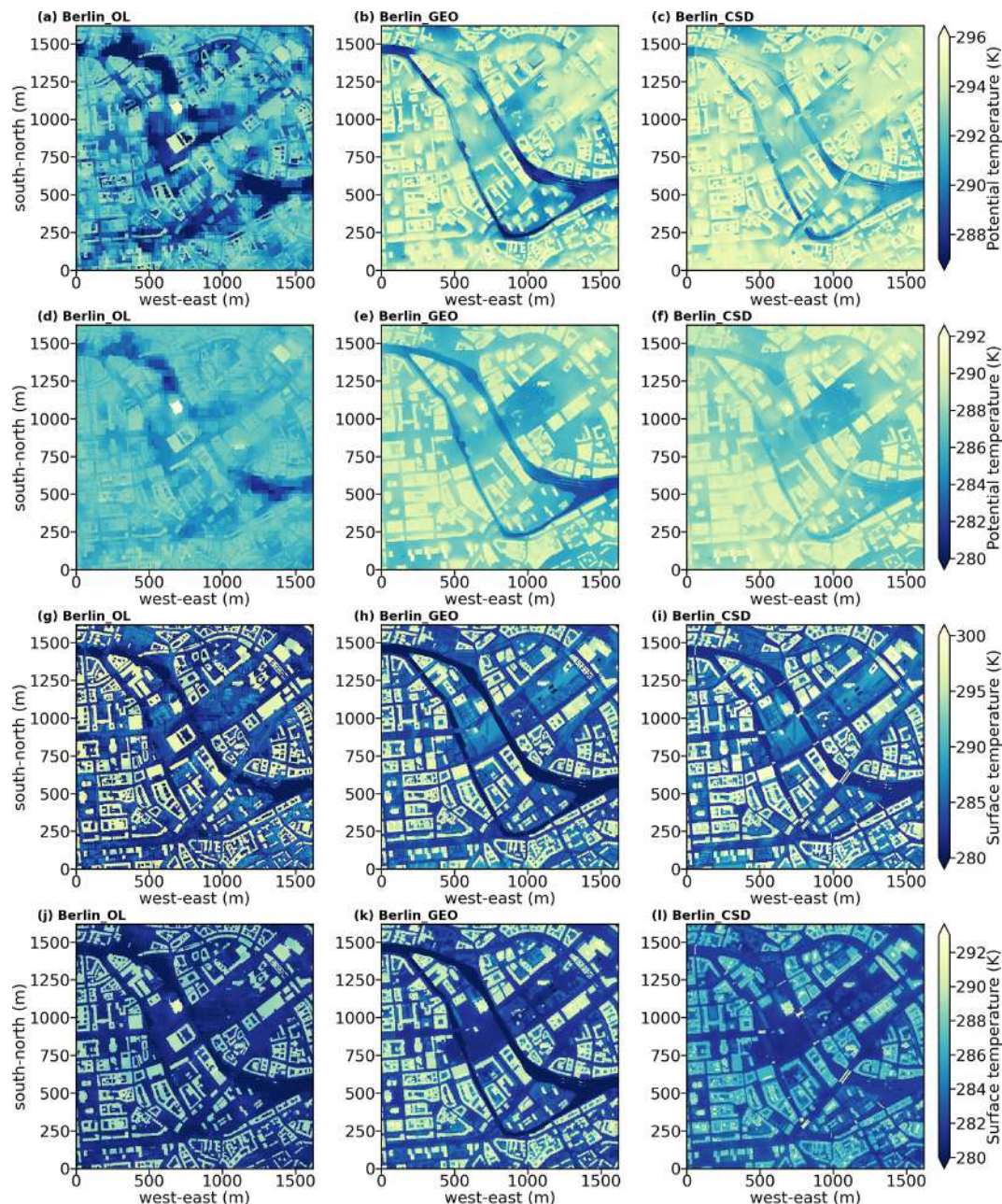
Figure 6. Horizontal cross-sections of simulation results for the Berlin case: **(a–f)** potential temperature at 2 m (θ_{2m}) and **(g–l)** surface temperature (T_{sfc}). Panels **(a)**–**(c)** and panels **(g)**–**(j)** are averages of the second hour of the simulation. Panels **(d)**–**(f)** and panels **(j)**–**(l)** are averages of the last hour of the simulations. Refer to the panel labels for the corresponding simulation.

which aligns with the satellite image shown in Fig. 9a. Pavement type and street type are almost identical in Chch_OL (Fig. 10d and g) and Chch_GEO (Fig. 10e and h) as they both used OSM data. The OSM data used in Chch_OL may be more up to date, while Chch_GEO used local data that were processed and checked manually. In GEO4PALM, the OSM interface recognised the footpath on the Westfield Riccarton rooftop car park as pavements. GEO4PALM removes the buildings if they overlap with pavements, whereas

PALM CSD removes the pavements when they overlap with buildings. More investigation is needed to determine a more appropriate overlap check. However, in this case, the removal of buildings could be problematic. Comparing Fig. 10j to Fig. 10k, Chch_OL has several buildings missing. Since Chch_GEO was sourced from both OSM and the NZ Building Outlines data set (Land Information New Zealand, 2020), its building information is more comprehensive and accurate. In addition, similarly to the Berlin case, OSM online
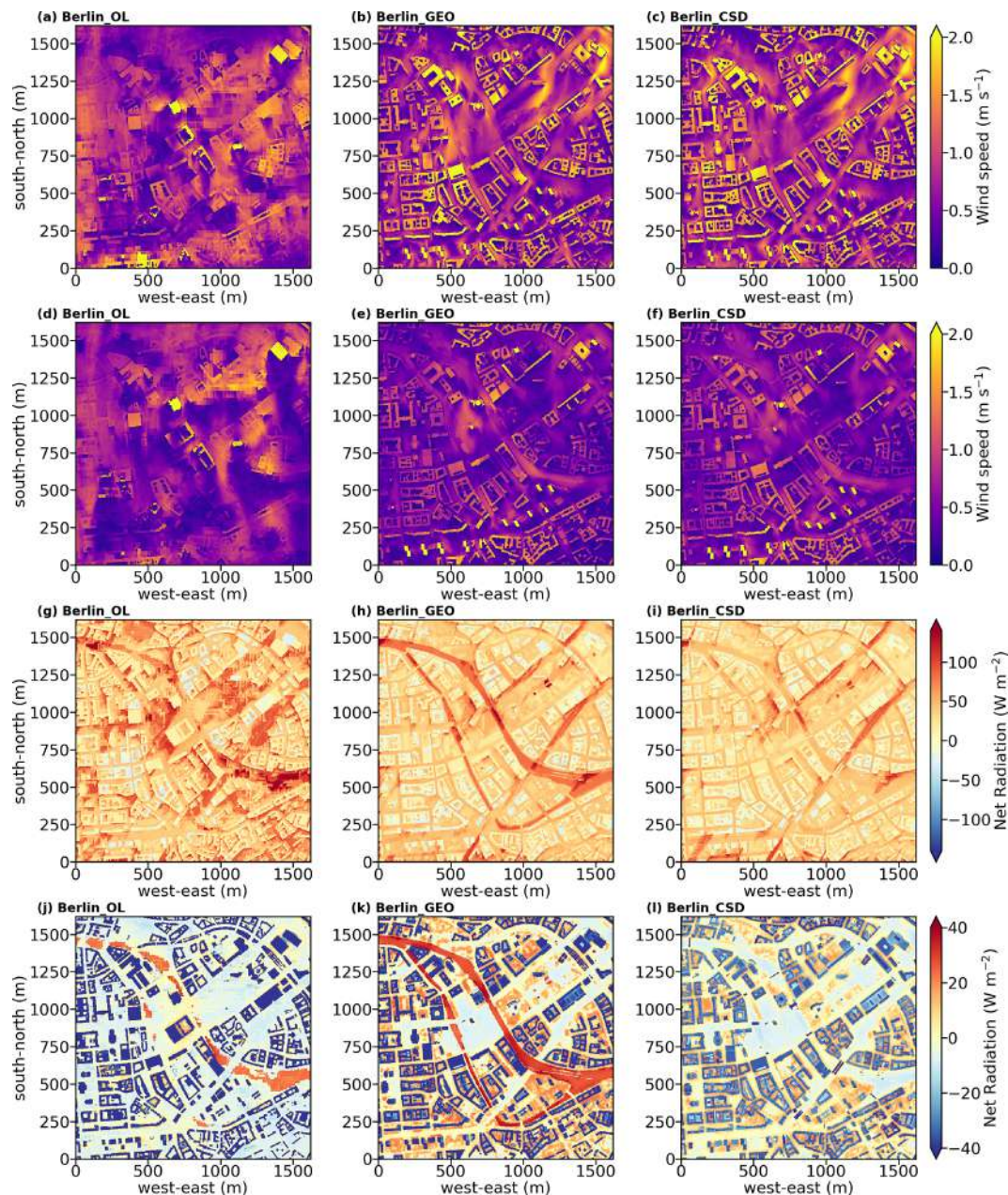
Figure 7. Similar to Fig. 6 but for wind speed at $10\,\text{m}$ ($WS_{10\,\text{m}}$) **(a–f)**, and surface net radiation (R_{net}) **(g–l)**. Refer to the panel labels for the corresponding simulation.

data do not provide much building height information, and hence, most buildings in Chch_OL have a dummy height of $3\,\text{m}$ (Fig. 10j).

Using the same input files, the static driver input created by GEO4PALM and PALM CSD are almost identical. The LAI input for PALM CSD is derived using the LAI calculated by GEO4PALM. In other words, the LAI shown in Fig. 9c for Chch_CSD used the LAI shown in Fig. 9b for Chch_GEO as an input. Since PALM CSD applies adjustments to the vegetation type (see Fig. 10b–c) and checks the

resolved plant canopy and its underlying vegetation types, the LAI in Chch_CSD is only present over areas where the vegetation type is not bare soil (see Fig. 9c).

Simulation results for the Ōtautahi / Christchurch case are shown in Figs. 11, 12, and 13. Similarly to the Berlin case, due to the coarse resolution of the input topography data, Chch_OL presents results with box-like structures, especially over the sports fields to the north of Riccarton Bush, where the land is exposed with no surface objects like buildings and plant canopies. The impact of the plant
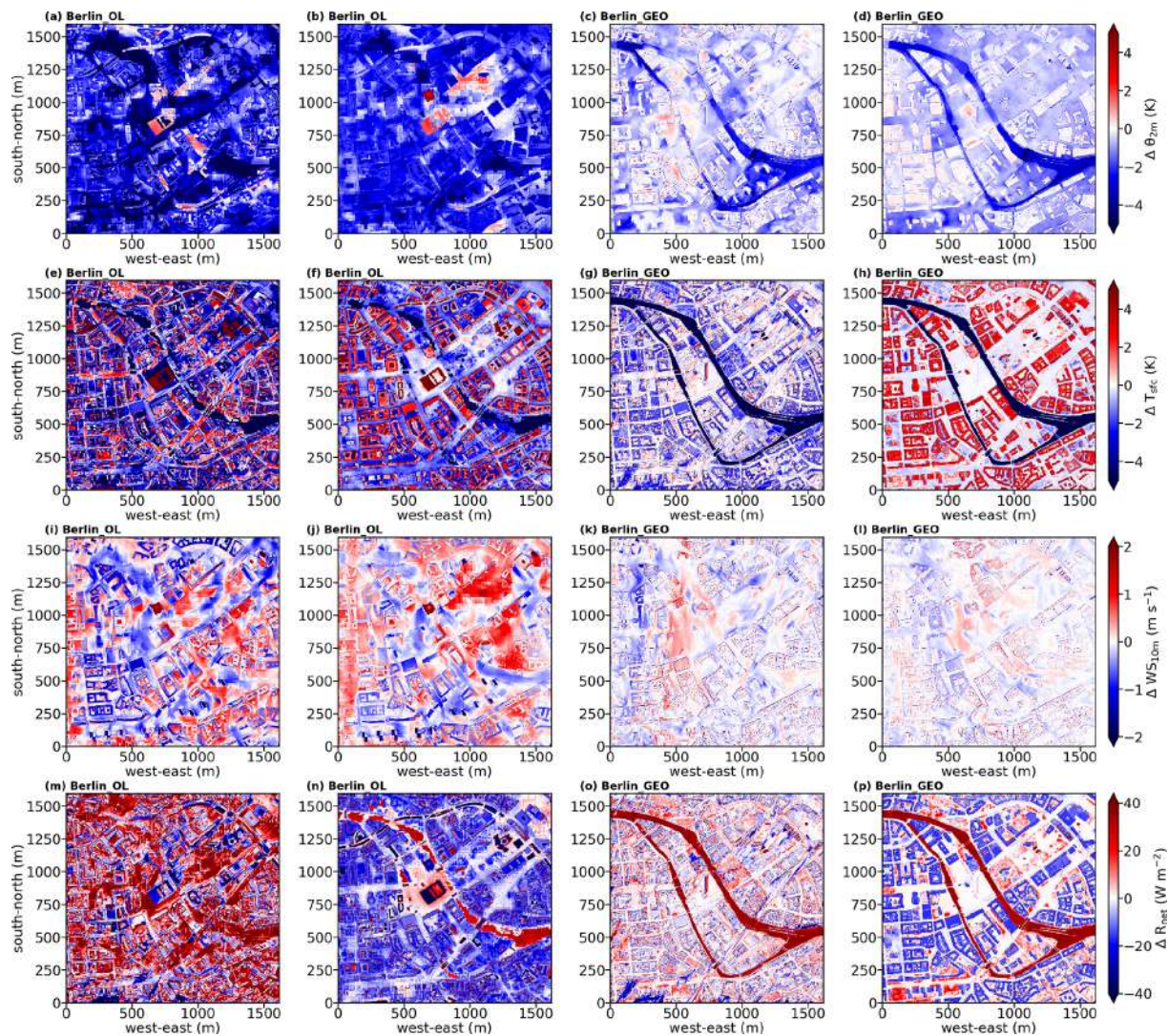
Figure 8. Differences in simulation results (shown in Figs. 6 and 7) between GEO4PALM simulations and PALM CSD simulation. The differences are results of GEO4PALM simulations subtracted from the PALM CSD simulation: **(a–d)** differences in θ_{2m}, **(e–h)** differences in T_{sfc}, **(i–l)** differences in $WS_{10\,m}$, and **(m–p)** differences in R_{net}. From left to right, the first and the second columns show the differences between Berlin_OL and Berlin_CSD for the second and sixth hour of the simulations, respectively. The third and fourth columns show the differences between Berlin_GEO and Berlin_CSD for the second and sixth hour of the simulations, respectively. Refer to the panel labels for the corresponding simulation.

canopies is noticeable in Chch_GEO and Chch_OL. In contrast to Chch_OL, Chch_GEO presents lower θ_{2m} (Fig. 11a–f) and T_{sfc} (Fig. 11g–l) over the plant canopies. Compared to Chch_CSD, the different configuration of vegetation types in Chch_OL introduces a warm bias in θ_{2m} (Fig. 11a–b) and a cold bias in T_{sfc} (Fig. 11g and h) over the areas which Chch_OL recognises as vegetation rather than bare soil. The area with missing buildings in Chch_OL is colder than that in Chch_CSD (Fig. 11a–b). Over the Riccarton Bush area, Chch_OL does not have a resolved plant canopy, which leads to an overestimation of T_{sfc} in the area in the last hour of the simulations (Fig. 13f), while most areas of the domain coincide with a cold bias in T_{sfc} compared to Chch_CSD. In addi-

tion to the missing plant canopy, the lack of building heights leads to a significant overestimation of $WS_{10\,m}$ in Chch_OL in the second and the last hours of the simulations (Fig. 13i–j). The problem of lacking plant and urban canopies is more evident for R_{net} in Chch_OL. As shown in Fig. 13m, the differences in R_{net} are positive where the buildings and the resolved plant canopies are not present in Chch_OL. In the last simulation hour, Chch_OL gives a positive bias in R_{net} for most areas of the domain (Fig. 13n). These results, again, highlight the importance of accurate input geospatial data.

Comparing Chch_GEO to Chch_CSD, the resolved plant canopy plays a major role in the differences between the simulations. The presence of a denser plant canopy over Riccar-

Table 6. Geospatial input data for GEO4PALM used in the Ōtautahi / Christchurch case study.

GEO4PALM variables	Data set	Source
	Chch_GEO	
water	GHRSST Level-4 MUR product	OPeNDAP via Earthdata (https://lpdaac.usgs.gov/tools/opendap/; last access: 7 November 2023)
dem	Ōtautahi / Christchurch DEM with spatial resolution of 1 m	Envirionment Canterbury Regional Council (2020)
lu	New Zealand LCDB v5.0	Refer to Landcare Research (2020)
bldh	– OSM – Ōtautahi / Christchurch DEM with spatial resolution of 1 m – Ōtautahi / Christchurch DSM with spatial resolution of 1 m – NZ Building Outlines data set	– OpenStreetMap – Envirionment Canterbury Regional Council (2020) – Land Information New Zealand (2020)
bldid	OSM	OpenStreetMap
pavement	OSM	OpenStreetMap
street	OSM	OpenStreetMap
sfch	– Ōtautahi / Christchurch DEM with spatial resolution of 1 m – Ōtautahi / Christchurch DSM with spatial resolution of 1 m	Envirionment Canterbury Regional Council (2020)
water	GHRSST Level-4 MUR product	OPeNDAP via Earthdata (https://lpdaac.usgs.gov/tools/opendap/; last access: 7 November 2023)
dem	NASA Shuttle Radar Topography Mission 1 arcsec NetCDF V003 (SRTMGL1_NC.003)	A$\rho\rho$EEARS (https://appeears.earthdatacloud.nasa.gov/; last access: 7 November 2023)
lu	ESA WorldCover 10 m (2020 V1)	TerraCatalogueClient (https://vitobelgium.github.io/terracatalogueclient; last access: 7 November 2023)
bldh	OSM	OpenStreetMap via OSMnx (Boeing, 2017)
bldid	OSM	OpenStreetMap via OSMnx (Boeing, 2017)
pavement	OSM	OpenStreetMap via OSMnx (Boeing, 2017)
street	OSM	OpenStreetMap via OSMnx (Boeing, 2017)
sfch	Not available	Not applicable

ton Bush in Chch_GEO leads to a cold bias in θ_{2m} and T_{sfc} in both the second and the last simulation hours (Fig. 13c–d and g–h). In the second simulation hour, with more resolved plant canopies in the simulation domain, Chch_GEO gives a higher θ_{2m} and a lower T_{sfc} (Fig. 13c and g). In the last simulation hour, the impact of plant canopies on θ_{2m} is significant in that the colder areas in Chch_GEO (Fig. 13d) align with the high-LAI areas shown in Fig. 9b. The increase in surface roughness due to the presence of the denser plant canopies in Chch_GEO also introduces a considerable decrease in wind speed compared to Chch_CSD (Fig. 13k–l). In addition, the R_{net} in Chch_GEO is generally lower across the entire simu-

lation domain than that in Chch_CSD (Fig. 13o–p). The differences between Chch_GEO and Chch_CSD agree with the assumption that, without the vegetation-type adjustment and with a potentially overestimated LAD, the simulation will create biases, especially in the simulated winds. These differences are evident in the Ōtautahi / Christchurch case because of low buildings and a higher proportion of the resolved plant canopies. In the Berlin case, the tallest building is 123.6 m with a domain-averaged building height of 23.9 m. The highest building in the Ōtautahi / Christchurch case is only 25.0 m high, and the domain-averaged building height is 4.8 m, while most of the trees in Riccarton Bush are over
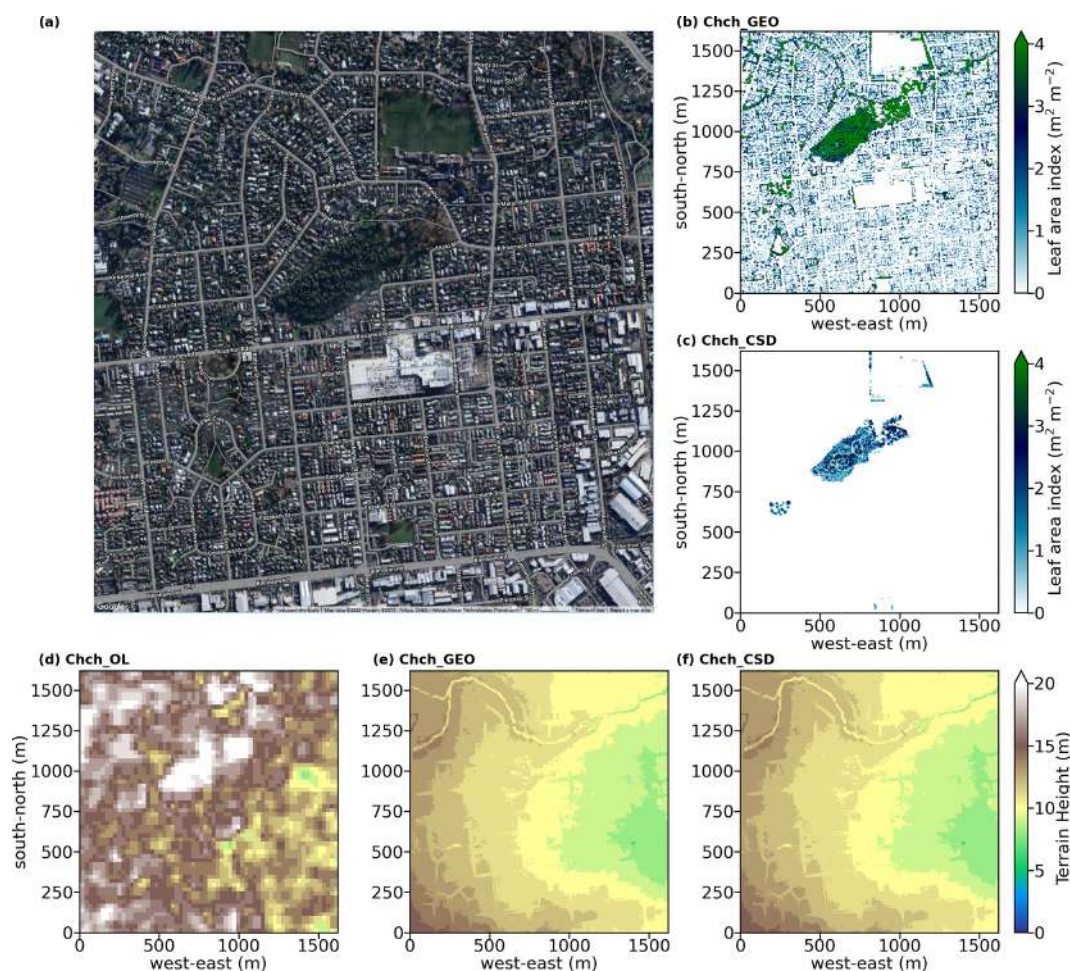
Figure 9. Similar to Fig. 4 but for the Ōtautahi / Christchurch case. Domain centre is located near Riccarton Bush in Ōtautahi / Christchurch, New Zealand (satellite image © Google Earth). Refer to the panel label for the corresponding simulation. For data sources refer to Table 6.

12.0 m high. Therefore, in the Ōtautahi / Christchurch case, the vegetation is the main surface forcing, and such forcing could alter the simulation results significantly.

5 Conclusions

This study presents GEO4PALM, a utility written in Python that generates PALM static driver input for the PALM model system. With GEO4PALM, PALM users now have the freedom to create static drivers with any geospatial data they have and/or the online data provided. Two application examples were given to demonstrate the applicability of GEO4PALM. The results show that GEO4PALM is a useful tool to realise near-surface microscale structures. When the same geospatial input data are used, the GEO4PALM static drivers can present simulation results comparable to the PALM CSD static drivers. There are differences between the results generated by the two tools. However, without validations against observational data, we cannot verify which tool's approach

is more appropriate. The optimal simulation setup needs to be investigated in future simulations and experiments along with observational data. To the best of our knowledge, current static driver generation tools in the PALM community (PALM CSD, palmpy, and PALM-4U GUI) either heavily rely on users to pre-process geospatial data or have not been applied to many regions in the world, for example, New Zealand. GEO4PALM simplifies data acquisition by automating and standardising data pre-processing and conversion. The online data interfaces, automatic projection conversion, and translation of land cover classes make GEO4PALM a widely applicable tool. These features, however, have not yet been implemented in PALM CSD. In addition to the static driver generation code, GEO4PALM provides a GUI for users to visualise and configure the simulation domains easily.
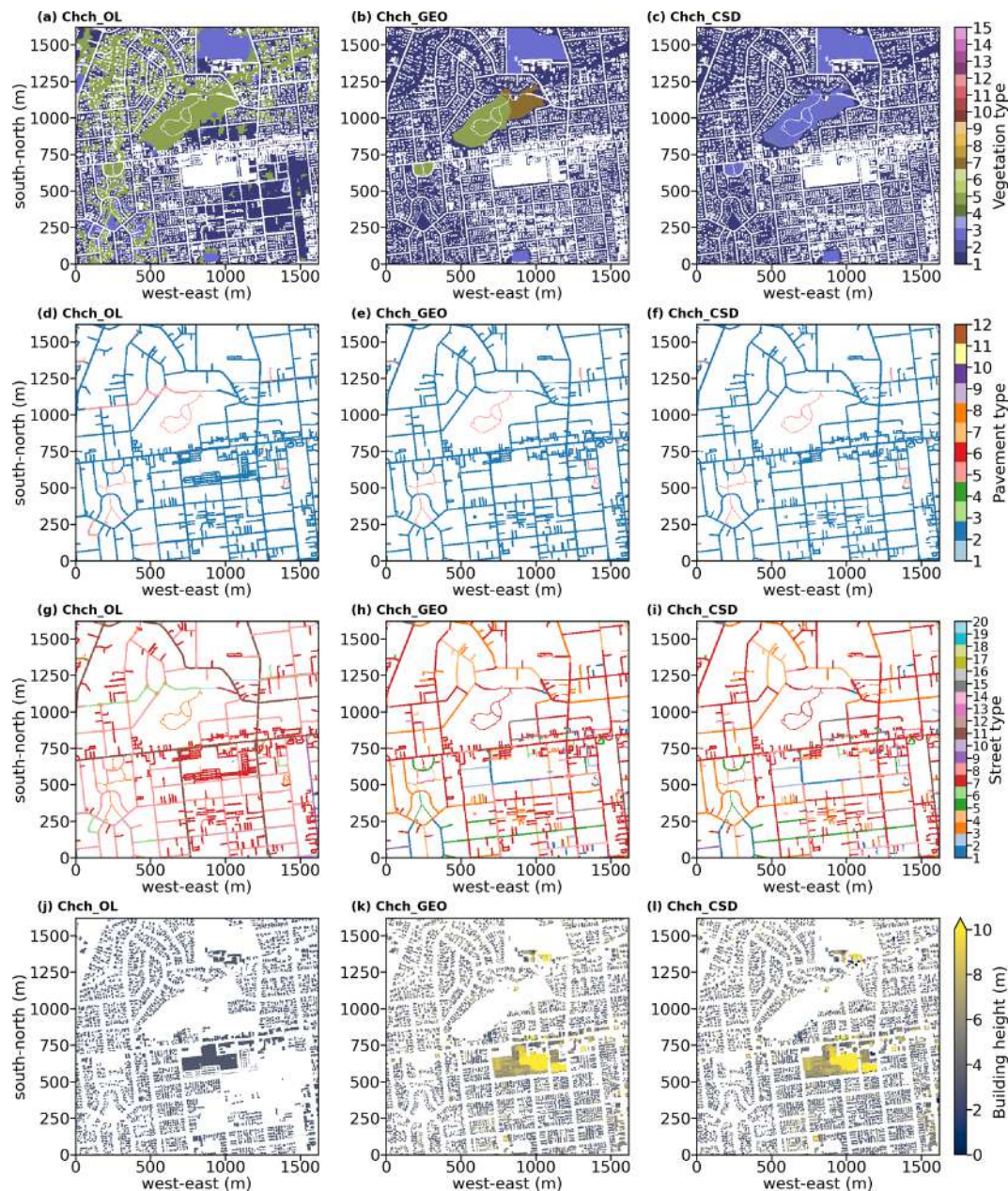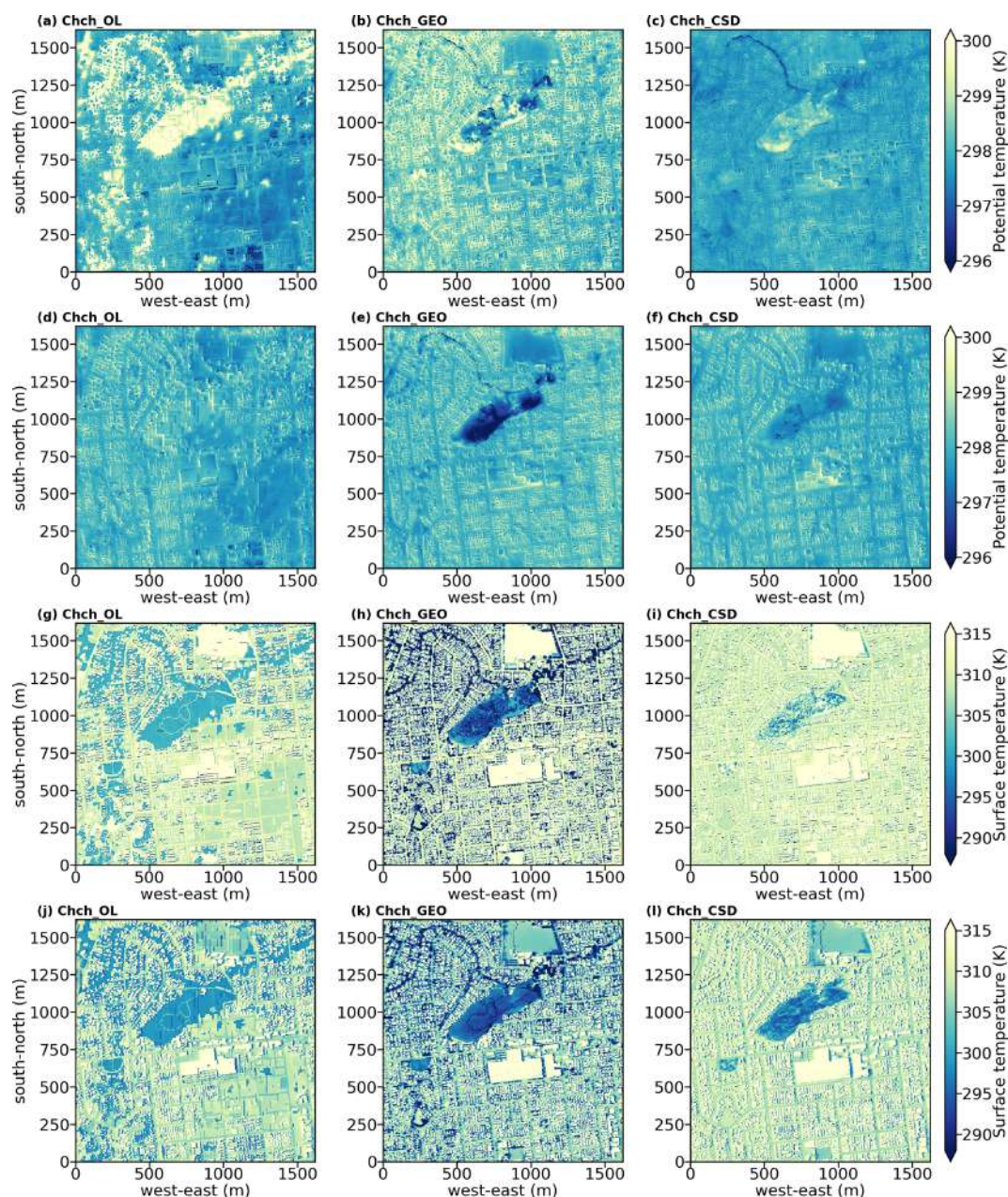
Figure 10. Similar to Fig. 5 but for the Ōtautahi / Christchurch case. Refer to the panel label for the corresponding simulation. For data sources refer to Table 6.

5.1 Limitations

GEO4PALM is developed as a free, open-source, and community-driven tool and is distributed on GitHub (https://github.com/dongqi-DQ/GEO4PALM; last access: 7 November 2023). As discussed, GEO4PALM does not cover all the variables in the static driver of the PALM model system. The fidelity and features of static driver input depend on the input geospatial data quality and availability, which have been a particular challenge when conducting microscale simulations. GEO4PALM provides several interfaces for users to

download global geospatial data sets, which include the basic features of PALM static input, such as topography and land use typology. However, as shown in the case studies, these online data sets are of coarse resolution and are not suitable for high-resolution urban applications at the metre scale. These online data sets could be handy for quickly conducting simulations over a large area with coarse resolutions. The building height and plant canopy information are currently missing in the online data sets covered by GEO4PALM. The LAD estimation method in GEO4PALM may lead to biases in simulations for highly vegetated areas. High-resolution
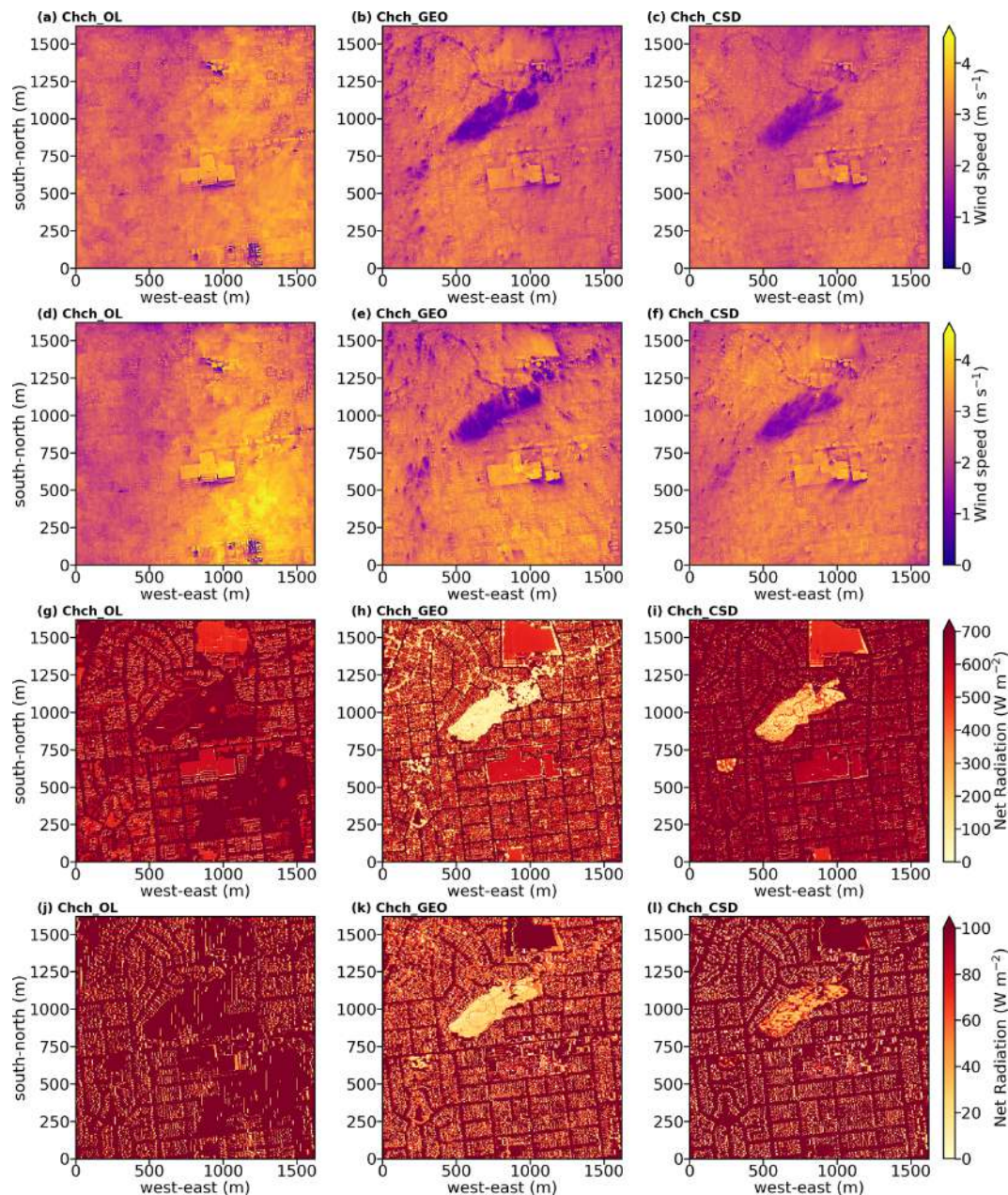
Figure 11. Similar to Fig. 6 but for the Ōtautahi / Christchurch case. Refer to the panel label for the corresponding simulation.

building-type and water temperature data sets are currently not included in GEO4PALM, while these data sets are not publicly available. In addition, GEO4PALM does not apply any adjustments to vegetation types and/or topography. Whether the adjustments would improve the simulations requires further investigation, which is out of the scope of this paper but should be considered in future developments of GEO4PALM.

5.2 Outlook

Many regions worldwide do not have high-resolution geospatial data to realise simulations with high fidelity. High-resolution building height data are important for urban applications, but they are not widely available, making simulations over human settlement difficult. While building height information could sometimes be obtained from the local authorities in large cities, the availability of such data sets might vary depending on the regions of interest. Additionally, for research purposes, there might be differences in ac-
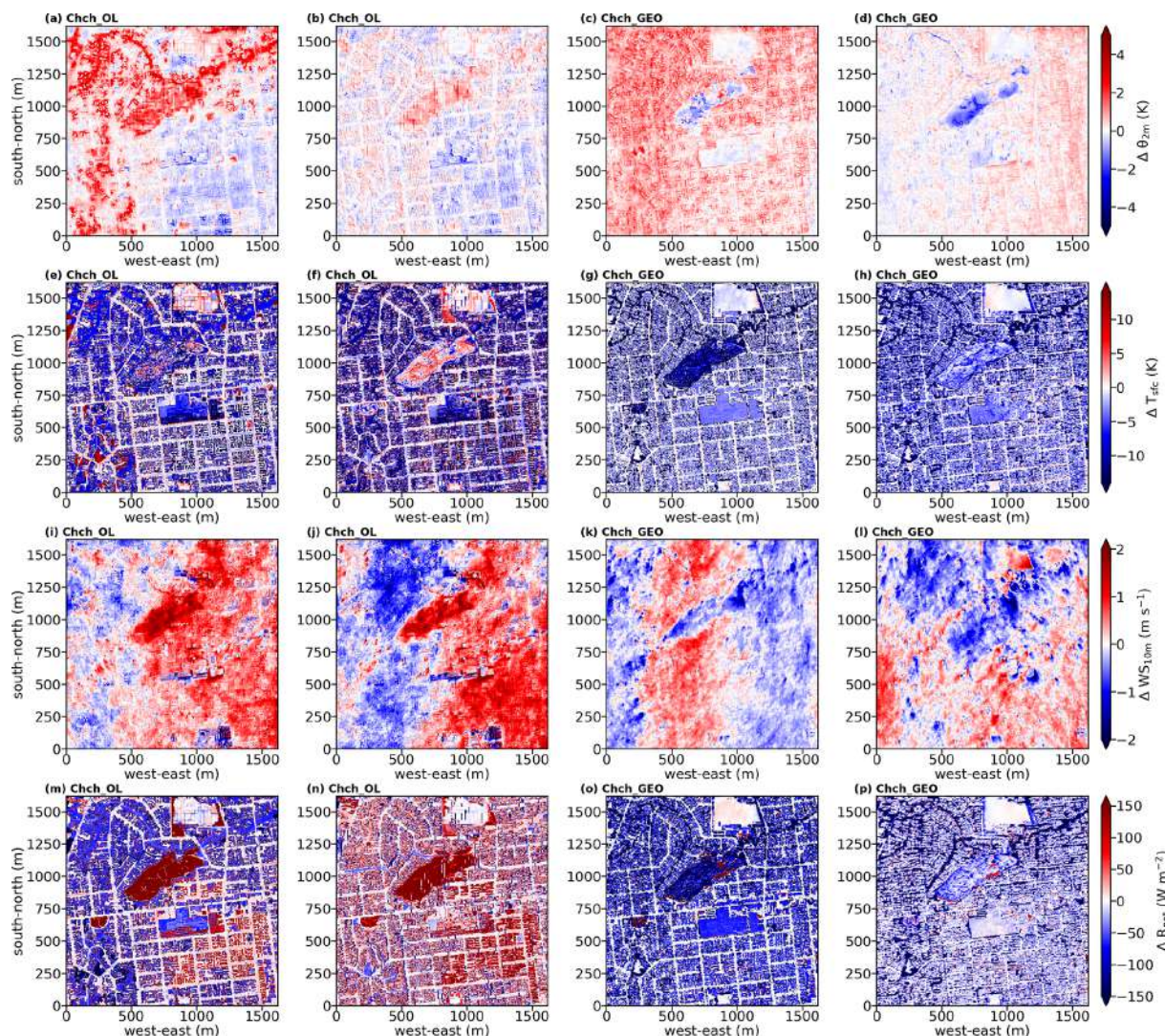
Figure 12. Similar to Fig. 7 but for the Ōtautahi / Christchurch case. Refer to the panel label for the corresponding simulation.

cessibility and cost, particularly in smaller or less developed areas. Fortunately, with increasing efforts towards research at the microscale, especially urban climate research, new data sets have been developed for microscale simulations. For example, high-resolution geospatial data can be obtained from Geoscape (https://geoscape.com.au/; last access: 7 November 2023) for applications in Australia. Microsoft provides AI-assisted building footprint mapping (https://www.microsoft.com/en-us/maps/building-footprints; last access: 7 November 2023). Using a deep neural network, the GLObal Building heights for Urban Studies (GLOBUS)

gives a novel Level of Detail-1 (LoD-1) building data set (Kamath et al., 2022). Esch et al. (2022) presented World Settlement Footprint 3D, which provides three-dimensional morphology and density of buildings worldwide. Some of these data sets are not freely available or need to be acquired based on individual requests, while GEO4PALM accepts all geospatial data in GeoTIFF format. Once users have obtained the data sets they desire, GEO4PALM is able to process such data for PALM simulations.

Another common challenge in land use data sets is that many land use classification data sets only classify urban ar-

Figure 13. Similar to Fig. 8 but for the Ōtautahi / Christchurch case. Refer to the panel label for the corresponding simulation.

eas into a limited number of typologies. This could lead to a loss of fidelity. Lipson et al. (2022) have described a data transformation method to make the urban land use data more descriptive. This may potentially improve the quality of land use classification data sets, for example, for applications in New Zealand, where only one type of land use was classified for urban areas. GEO4PALM currently only accepts vegetation heights as input for plant canopy due to a lack of geospatial data. In the future, we aim to improve this feature based on the PALM CSD tool (Heldens et al., 2020) and to include more data sources if available. While PALM CSD applies various checks on and modifications of the input geospatial data, e.g. topography and vegetation types, these features have not yet been implemented in GEO4PALM. As shown in the Ōtautahi / Christchurch case study, the vegetation-type adjustments could substantially impact the simulation results. Furthermore, this paper only compared GEO4PALM

to PALM CSD, while palmpy and PALM-4U GUI are other tools that could have more advanced features. Hence, in addition to the investigation and development of vegetation-type adjustment, future work may also include a comparison between the four tools for better improvements to GEO4PALM.

GEO4PALM accepts any geospatial data sets as input and is easily adaptive to new data downloading interfaces. With the development of geospatial data sets towards better spatial coverage and data quality, GEO4PALM can be improved and extended. All PALM users are encouraged to provide feedback and report bugs and issues via the issue system provided by GitHub. Any optimisation of, modification of, or contribution to the code is welcome and much appreciated.

Appendix A: GEO4PALM step-by-step guide

A more detailed user manual is available at https://github.com/dongqi-DQ/GEO4PALM (last access: 7 November 2023).

A1   Step 1: prepare configuration file

The configuration file should be provided in the `./JOBS/case_name/` folder as follows:

```
[case]
case_name          - name of the case
origin_time        - date and time at model start*
default_proj       - default is EPSG:4326. This projection uses lat/long to
                     locate domain. This may not be changed.
config_proj        - projection of input .tif files. GEO4PALM will automatically assign
                     the UTM zone if not provided.
                     We recommend users use local projection with units in metres;
                     e.g. for New Zealand users, EPSG:2193 is a recommended choice.
lu_table           - land use lookup table to convert land use classification
                     to PALM recognisable


[settings]
water_temperature     - user input water temperature values when
                        no water temperature data are available
building_height_dummy - user input dummy height for buildings
                        where building heights are missing in the
                        OSM data set or if building heights are
                        0.0 m in the input data
tree_height_filter    - user input to filter small objects; i.e., if
                        object height is smaller than this value,
                        then this object is not included in the LAD estimation


[domain]
ndomain            - maximum number of domains, when >=2, domain nesting is enabled
centlat, centlon   - centre latitude and longitude of the first domain. Note this is
                     not required for nested domains
nx                 - number of grid points along the x axis
ny                 - number of grid points along the y axis
nz                 - number of grid points along the z axis
dx                 - grid spacing in metres along the x axis
dy                 - grid spacing in metres along the y axis
dz                 - grid spacing in metres along the z axis
z_origin           - elevated terrain mean grid position in metres
                     (leave as 0.0 if unknown)
ll_x               - lower-left corner distance to the first domain in
                      metres along x axis
ll_y               - lower-left corner distance to the first domain in
                     metres along y axis


[geotif]           - required input from the user; can be provided by users
                     in the INPUT folder or "online"
water              -  input for water temperature
dem                - digital elevation model input for topography
lu                 - land use classification
```

```
resample_method   -  method to resample GeoTIFF files for interpolation/extrapolation

# if NASA API is used format in YYYY-MM-DD
# SST date should be the same as the orignin_time

## No need to change start/end dates for NASA SRTMGL1_NC.003
dem_start_date = '2000-02-12',
dem_end_date = '2000-02-20',
## start/end dates for land use data set
lu_start_date = '2020-10-01',
lu_end_date = '2020-10-30',

[urban]             - input for urban canopy model; can leave as "" if this
                      feature is not included in the simulations, or provided by
                      users or online from OSM
bldh                - input for building height
bldid               - input for building ID
pavement            - input for pavement type
street              - input for street type

[plant]             - input for plant canopy model; can leave as "" if this
                      feature is not included in the simulations,
                      or provided by users
tree_lai_max        - input value for maximum leaf area index (LAI)
lad_max_height      - input value for the height where the leaf area density (LAD)
                       reaches LADm
sfch                - input for plant height; this is for leaf area density (LAD)
```

A2   Step 2: provide input files where applicable

Move   all   input   geospatial   data   to   the `./JOBS/case_name/INPUT` folder.

A3   Step 3: run the main script

```
python run_config_static.py case_name
```

Appendix B: Land use type lookup table

Table B1. Lookup table to convert NASA LC_Type01 classes to PALM vegetation type, pavement type, building type, water type, and soil type.

Class code	Class name	Vegetation type	Pavement type	Building type	Water type	Soil type
1	Evergreen needleleaf forests	4				5
2	Evergreen broadleaf forests	6				5
3	Deciduous needleleaf forests	5				5
4	Deciduous broadleaf forests	7				5
5	Mixed forests	17				5
6	Closed shrublands	15				5
7	Open shrublands	16				5
8	Woody savannas	17				4
9	Savannas	17				4
10	Grasslands	8				3
11	Permanent wetlands	14				6
12	Croplands	11				4
13	Urban and built-up lands			3		
14	Cropland/natural vegetation mosaics	2				5
15	Permanent snow and ice	13				1
16	Barren	12				1
17	Waterbodies				2	
255	Unclassified				2	
−9999	Not a number or no data				2	

Table B2. Lookup table to convert ESA WorldCover classes to PALM vegetation type, pavement type, building type, water type, and soil type.

Class code	Class name	vegetation type	Pavement type	Building type	Water type	Soil type
10	Tree cover	5				4
20	Shrubland	15				4
30	Grassland	3				3
40	Cropland	2				3
50	Built-up			3		
60	Bare/sparse vegetation	1				1
70	Snow and ice	13				1
80	Permanent waterbodies				2	
90	Herbaceous wetland	14				6
95	Mangroves	6				6
100	Moss and lichen	3				6
−9999	Not a number or no data				2	
255	Not a number or no data				2	

Table B3. Lookup table to convert NZ LCDB v5.0 classes to PALM vegetation type, pavement type, building type, water type, and soil type.

Class code	Class name	Vegetation type	Pavement type	Building type	Water type	Soil type
1	Built-up area (settlement)			3		
2	Urban parkland/open space	3				3
5	Transport infrastructure		3			1
6	Surface mine or dump	1				1
10	Sand or gravel	1				1
11	River and lakeshore gravel and rock				2	
12	Landslide	1				1
13	Alpine gravel and rock	1				1
14	Permanent snow and ice	1				1
15	Alpine grass/herbfield	3				6
16	Gravel or rock	1				1
20	Lake or pond				1	
21	River				2	
22	Estuarine open water				2	
30	Short-rotation cropland	2				6
33	Orchards, vineyards, or other perennial crops	11				6
40	High-producing exotic grassland	3				6
41	Low-producing grassland	3				6
43	Tall tussock grassland	8				6
44	Depleted grassland	3				1
45	Herbaceous freshwater vegetation	14				6
46	Herbaceous saline vegetation	16				6
47	Flaxland	8				6
50	Fernland	3				6
51	Gorse and/or broom	8				6
52	Manuka and/or kanuka	8				6
54	Broadleaved indigenous hardwoods	7				6
55	Sub-alpine shrubland	15				6
56	Mixed exotic shrubland	15				6
58	Matagouri or grey scrub	8				6
60	Minor shelterbelts	18				6
61	Major shelterbelts	18				6
64	Forest – harvested	17				6
68	Deciduous hardwoods	5				6
69	Indigenous forest	6				6
70	Mangrove	14				6
71	Exotic forest	7				6
−9999	Not a number or no data				2	

Author contributions. DL was responsible for the data acquisition, conceptualisation of the GEO4PALM tool, initial and major development of GEO4PALM, GEO4PALM code distribution and documentation, conducting PALM simulations, formal analysis, and visualisation. JZ contributed to the conceptualisation of GEO4PALM v1.1, major GEO4PALM development, and GEO4PALM documentation and developed the PALM domain utility GUI. BK provided the DLR data sets and contributed to the conceptualisation of case studies. DL wrote the manuscript with contributions from JZ, BK, MK, and LER. DL, JZ, BK, MK, and LER reviewed the manuscript.

Competing interests. The contact author has declared that none of the authors has any competing interests.

Disclaimer. Publisher's note: Copernicus Publications remains neutral with regard to jurisdictional claims made in the text, published maps, institutional affiliations, or any other geographical representation in this paper. While Copernicus Publications makes every effort to include appropriate place names, the final responsibility lies with the authors.

Review statement. This paper was edited by Simone Marras and reviewed by two anonymous referees.

References

Belda, M., Resler, J., Geletič, J., Krč, P., Maronga, B., Sühring, M., Kurppa, M., Kanani-Sühring, F., Fuka, V., Eben, K., Benešová, N., and Auvinen, M.: Sensitivity analysis of the PALM model system 6.0 in the urban environment, Geosci. Model Dev., 14, 4443–4464, https://doi.org/10.5194/gmd-14-4443-2021, 2021.

Boeing, G.: OSMnx: New methods for acquiring, constructing, analyzing, and visualizing complex street networks, Computers, Environment and Urban Systems, 65, 126–139, Elsevier, ISBN 0198-9715 2017.

Bou-Zeid, E., Meneveau, C., and Parlange, M. B.: Large-eddy simulation of neutral atmospheric boundary layer flow over heterogeneous surfaces: Blending height and effective surface roughness, Water Resour. Res., 40, W02505, https://doi.org/10.1029/2003WR002475, 2004.

Chin, T. M., Vazquez-Cuervo, J., and Armstrong, E. M.: A multi-scale high-resolution analysis of global sea surface temperature, Remote Sens. Environ., 200, 154–169, https://doi.org/10.1016/j.rse.2017.07.029, 2017.

Envirionment Canterbury Regional Council: Christchurch and Ashley River, Canterbury, New Zealand 2018, https://doi.org/10.5069/G91J97WQ, 2020.

Esch, T., Brzoska, E., Dech, S., Leutner, B., Palacios-Lopez, D., Metz-Marconcini, A., Marconcini, M., Roth, A., and Zeidler, J.: World Settlement Footprint 3D – A first three-dimensional sur-

vey of the global building stock, Remote Sens. Environ., 270, 112877, https://doi.org/10.1016/j.rse.2021.112877, 2022.

Fluck, S.: Bodenturbulenzen um Flugplätze, Durchführung und Benchmarking von Turbulenzsimulationen Sowie Entwicklung eines Frameworks für zukünftige Problemstellungen, Master's Thesis, Zurich University of Applied Sciences, 2020.

Friedl, M. and Sulla-Menashe, D.: MCD12Q1 MODIS/Terra+Aqua Land Cover Type Yearly L3 Global 500m SIN Grid V006, NASA EOSDIS Land Processes Distributed Active Archive Center [data set], https://doi.org/10.5067/MODIS/MCD12Q1.006, 2019.

Gehrke, K. F., Sühring, M., and Maronga, B.: Modeling of land–surface interactions in the PALM model system 6.0: land surface model description, first evaluation, and sensitivity to model parameters, Geosci. Model Dev., 14, 5307–5329, https://doi.org/10.5194/gmd-14-5307-2021, 2021.

Gillies, S. et al.: Rasterio: geospatial raster I/O for Python programmers [software], https://github.com/rasterio/rasterio (last access: 29 January 2024), 2019.

Gronemeier, T., Raasch, S., and Ng, E.: Effects of Unstable Stratification on Ventilation in Hong Kong, Atmosphere, 8, 168, https://doi.org/10.3390/atmos8090168, 2017.

Heldens, W., Burmeister, C., Kanani-Sühring, F., Maronga, B., Pavlik, D., Sühring, M., Zeidler, J., and Esch, T.: Geospatial input data for the PALM model system 6.0: model requirements, data sources and processing, Geosci. Model Dev., 13, 5833–5873, https://doi.org/10.5194/gmd-13-5833-2020, 2020.

Hoyer, S. and Hamman, J.: xarray: ND labeled arrays and datasets in Python, J. Open Res. Softw., 5, 10, https://doi.org/10.5334/jors.148, 2017.

Jordahl, K., den Bossche, J. V., Fleischmann, M., Wasserman, J., McBride, J., Gerard, J., Tratner, J., Perry, M., Badaracco, A. G., Farmer, C., Hjelle, G. A., Snow, A. D., Cochran, M., Gillies, S., Culbertson, L., Bartos, M., Eubank, N., maxalbert, Bilogur, A., Rey, S., Ren, C., Arribas-Bel, D., Wasser, L., Wolf, L. J., Journois, M., Wilson, J., Greenhall, A., Holdgraf, C., Filipe, and Leblanc, F.: geopandas/geopandas: v0.8.1, Zenodo [software], https://doi.org/10.5281/zenodo.3946761, 2020.

Kamath, H. G., Singh, M., Magruder, L. A., Yang, Z.-L., and Niyogi, D.: GLOBUS: GLObal Building heights for Urban Studies, arXiv [preprint], https://doi.org/10.48550/arXiv.2205.12224, 24 May 2022.

Khan, B., Banzhaf, S., Chan, E. C., Forkel, R., Kanani-Sühring, F., Ketelsen, K., Kurppa, M., Maronga, B., Mauder, M., Raasch, S., Russo, E., Schaap, M., and Sühring, M.: Development of an atmospheric chemistry model coupled to the PALM model system 6.0: implementation and first applications, Geosci. Model Dev., 14, 1171–1193, https://doi.org/10.5194/gmd-14-1171-2021, 2021.

Knoop, H.: PALM Model System 22.10, https://gitlab.palm-model.org/releases/palm_model_system/-/releases/v22.10, last access: 29 January 2024.

Knoop, H., Sühring, M., and Raasch, S.: PALM Model System, https://gitlab.palm-model.org/releases/palm_model_system, last access: 29 January 2024.

Kolic, B.: Forest ecoclimatology, University of Belgrade, 295 pp., 1978.

Krč, P., Resler, J., Sühring, M., Schubert, S., Salim, M. H., and Fuka, V.: Radiative Transfer Model 3.0 integrated into the PALM model system 6.0, Geosci. Model Dev., 14, 3095–3120, https://doi.org/10.5194/gmd-14-3095-2021, 2021.

Kurppa, M., Hellsten, A., Roldin, P., Kokkola, H., Tonttila, J., Auvinen, M., Kent, C., Kumar, P., Maronga, B., and Järvi, L.: Implementation of the sectional aerosol module SALSA2.0 into the PALM model system 6.0: model development and first evaluation, Geosci. Model Dev., 12, 1403–1422, https://doi.org/10.5194/gmd-12-1403-2019, 2019.

Kurppa, M., Roldin, P., Strömberg, J., Balling, A., Karttunen, S., Kuuluvainen, H., Niemi, J. V., Pirjola, L., Rönkkö, T., Timonen, H., Hellsten, A., and Järvi, L.: Sensitivity of spatial aerosol particle distributions to the boundary conditions in the PALM model system 6.0, Geosci. Model Dev., 13, 5663–5685, https://doi.org/10.5194/gmd-13-5663-2020, 2020.

Lalic, B. and Mihailovic, D. T.: An empirical relation describing leaf-area density inside the forest for environmental modeling, J. Appl. Meteorol., 43, 641–645, https://doi.org/10.1175/1520-0450(2004)043<0641:AERDLD>2.0.CO;2, 2004.

Land Information New Zealand: New Zealand Building Outlines (All Sources), https://data.linz.govt.nz/layer/101292-nz-building-outlines-all-sources/ (last access: 29 January 2024), 2020.

Landcare Research: LCDB v5.0 – Land Cover Database version 5.0, Mainland New Zealand, https://lris.scinfo.org.nz/layer/104400-lcdb-v50-land-cover-database-version-50-mainland-new-zealand/ (last access: 29 January 2024), 2020.

Lin, D. and Zhang, J.: dongqi-DQ/GEO4PALM: Fix LAI variable names for final production (v1.1.9_lai_fix), Zenodo [code], https://doi.org/10.5281/zenodo.10414751, 2023.

Lin, D., Khan, B., Katurji, M., Bird, L., Faria, R., and Revell, L. E.: WRF4PALM v1.0: a mesoscale dynamical driver for the microscale PALM model system 6.0, Geosci. Model Dev., 14, 2503–2524, https://doi.org/10.5194/gmd-14-2503-2021, 2021.

Lin, D., Katurji, M., Revell, L. E., Khan, B., and Sturman, A.: Investigating multiscale meteorological controls and impact of soil moisture heterogeneity on radiation fog in complex terrain using semi-idealised simulations, Atmos. Chem. Phys., 23, 14451–14479, https://doi.org/10.5194/acp-23-14451-2023, 2023.

Lipson, M. J., Nazarian, N., Hart, M. A., Nice, K. A., and Conroy, B.: A Transformation in City-Descriptive Input Data for Urban Climate Models, Front. Environ. Sci., 10, 866398, https://doi.org/10.3389/fenvs.2022.866398, 2022.

Liu, X., Abà, A., Capone, P., Manfriani, L., and Fu, Y.: Atmospheric disturbance modelling for a piloted flight simulation study of airplane safety envelope over complex terrain, Aerospace, 9, 103, https://doi.org/10.3390/aerospace9020103, 2022.

Mahrt, L. and Hristov, T.: Is the Influence of Stability on the Sea Surface Heat Flux Important?, J. Phys. Oceanogr., 47, 689–699, https://doi.org/10.1175/JPO-D-16-0228.1, 2017.

Maronga, B., Hartogensis, O. K., Raasch, S., and Beyrich, F.: The effect of surface heterogeneity on the structure parameters of temperature and specific humidity: A large-eddy simulation case study for the LITFASS-2003 experiment, Bound.-Lay. Meteorol., 153, 441–470, https://doi.org/10.1007/s10546-014-9955-x, 2014.

Maronga, B., Gryschka, M., Heinze, R., Hoffmann, F., Kanani-Sühring, F., Keck, M., Ketelsen, K., Letzel, M. O., Sühring, M., and Raasch, S.: The Parallelized Large-Eddy Simulation Model (PALM) version 4.0 for atmospheric and oceanic flows: model

formulation, recent developments, and future perspectives, Geosci. Model Dev., 8, 2515–2551, https://doi.org/10.5194/gmd-8-2515-2015, 2015.

Maronga, B., Banzhaf, S., Burmeister, C., Esch, T., Forkel, R., Fröhlich, D., Fuka, V., Gehrke, K. F., Geletič, J., Giersch, S., Gronemeier, T., Groß, G., Heldens, W., Hellsten, A., Hoffmann, F., Inagaki, A., Kadasch, E., Kanani-Sühring, F., Ketelsen, K., Khan, B. A., Knigge, C., Knoop, H., Krč, P., Kurppa, M., Maamari, H., Matzarakis, A., Mauder, M., Pallasch, M., Pavlik, D., Pfafferott, J., Resler, J., Rissmann, S., Russo, E., Salim, M., Schrempf, M., Schwenkel, J., Seckmeyer, G., Schubert, S., Sühring, M., von Tils, R., Vollmer, L., Ward, S., Witha, B., Wurps, H., Zeidler, J., and Raasch, S.: Overview of the PALM model system 6.0, Geosci. Model Dev., 13, 1335–1372, https://doi.org/10.5194/gmd-13-1335-2020, 2020.

Meyer, D. and Riechert, M.: Open source QGIS toolkit for the Advanced Research WRF modelling system, Environ. Model. Softw., 112, 166–178, https://doi.org/10.1016/j.envsoft.2018.10.018, 2019.

NASA/JPL: GHRSST Level 4 MUR Global Foundation Sea Surface Temperature Analysis (v4.1), PO.DAAC, https://doi.org/10.5067/GHGMR-4FJ04, 2015.

Powers, J. G., Klemp, J. B., Skamarock, W. C., Davis, C. A., Dudhia, J., Gill, D. O., Coen, J. L., Gochis, D. J., Ahmadov, R., Peckham, S. E., Grell, G. A., Michalakes, J., Trahan, S., Benjamin, S. G., Alexander, C. R., Dimego, G. J., Wang, W., Schwartz, C. S., Romine, G. S., Liu, Z., Snyder, C., Chen, F., Barlage, M. J., Yu, W., and Duda, M. G.: The Weather Research and Forecasting Model: Overview, System Efforts, and Future Directions, B. Am. Meteor. Soc., 98, 1717–1737, https://doi.org/10.1175/BAMS-D-15-00308.1, 2017.

Raasch, S. and Schröter, M.: PALM – A large-eddy simulation model performing on massively parallel computers, Meteorol. Z., 10, 363–372, https://doi.org/10.1127/0941-2948/2001/0010-0363, 2001.

Rabus, B., Eineder, M., Roth, A., and Bamler, R.: The shuttle radar topography mission – a new class of digital elevation models acquired by spaceborne radar, ISPRS J. Photogramm., 57, 241–262, https://doi.org/10.1016/S0924-2716(02)00124-7, 2003.

Resler, J., Krč, P., Belda, M., Juruš, P., Benešová, N., Lopata, J., Vlček, O., Damašková, D., Eben, K., Derbek, P., Maronga, B., and Kanani-Sühring, F.: PALM-USM v1.0: A new urban surface model integrated into the PALM large-eddy simulation model, Geosci. Model Dev., 10, 3635–3659, https://doi.org/10.5194/gmd-10-3635-2017, 2017.

Resler, J., Eben, K., Geletič, J., Krč, P., Rosecký, M., Sühring, M., Belda, M., Fuka, V., Halenka, T., Huszár, P., Karlický, J., Benešová, N., Ďoubalová, J., Honzáková, K., Keder, J., Nápravníková, Š., and Vlček, O.: Validation of the PALM model system 6.0 in a real urban environment: a case study in Dejvice, Prague, the Czech Republic, Geosci. Model Dev., 14, 4797–4842, https://doi.org/10.5194/gmd-14-4797-2021, 2021.

Rihani, J. F., Chow, F. K., and Maxwell, R. M.: Isolating effects of terrain and soil moisture heterogeneity on the atmospheric boundary layer: Idealized simulations to diagnose land-atmosphere feedbacks, J. Adv. Model. Earth Sy., 7, 915–937, https://doi.org/10.1002/2014MS000371, 2015.

Salim, M. H., Schubert, S., Resler, J., Krč, P., Maronga, B., Kanani-Sühring, F., Sühring, M., and Schneider, C.: Importance of radiative transfer processes in urban climate models: a study based on the PALM 6.0 model system, Geosci. Model Dev., 15, 145–171, https://doi.org/10.5194/gmd-15-145-2022, 2022.

Snow, A., BENR0, Cook, J., LiamRMoore, Taves, M., and Pierrick, R.: corteva/geocube: 0.2.0, Zenodo [software], https://doi.org/10.5281/zenodo.6399307, 2022a.

Snow, A., Brochart, D., Raspaud, M., Bell, R., Scott, R., Chegini, T., Amici, A., Braun, R., Annex, A., Hoese, D., Bunt, F., Ballesteros, G., Hamman, J., Zehner, M., Cordeiro, M., Henderson, S., Miller, S., Badger, G., Augspurger, T., Chantawibul, A., and Pmallas: corteva/rioxarray: 0.11.1, Zenodo [software], https://doi.org/10.5281/zenodo.6478182, 2022b.

Srivastava, A., Kumari, N., and Maza, M.: Hydrological Response to Agricultural Land Use Heterogeneity Using Variable Infiltration Capacity Model, Water Resour. Manage., 34, 3779–3794, https://doi.org/10.1007/s11269-020-02630-4, 2020.

Uni Hannover: PALM Create Static Driver (palm_csd), https://palm.muk.uni-hannover.de/trac/wiki/doc/app/iofiles/pids/palm_csd last access: 29 January 2024.

Vollmer, L., Lee, J. C.-Y., Steinfeld, G., and Lundquist, J. K.: A wind turbine wake in changing atmospheric conditions: LES and lidar measurements, J. Phys. Conf. Ser., 854, 012050, https://doi.org/10.1088/1742-6596/854/1/012050, 2017.

Wolf, T., Pettersson, L. H., and Esau, I.: A very high-resolution assessment and modelling of urban air quality, Atmos. Chem. Phys., 20, 625–647, https://doi.org/10.5194/acp-20-625-2020, 2020.

Wolf, T., Pettersson, L. H., and Esau, I.: Dispersion of particulate matter ($PM_{2.5}$) from wood combustion for residential heating: optimization of mitigation actions based on large-eddy simulations, Atmos. Chem. Phys., 21, 12463–12477, https://doi.org/10.5194/acp-21-12463-2021, 2021.

Zanaga, D., Van De Kerchove, R., De Keersmaecker, W., Souverijns, N., Brockmann, C.and Quast, R., Wevers, J., Grosu, A., Paccini, A., Vergnaud, S., Cartus, O., Santoro, M., Fritz, S., Georgieva, I., Lesiv, M., Carter, S., Herold, M., Li, L., Tsendbazar, N., Ramoino, F., and Arino, O.: ESA WorldCover 10 m 2020 v100, Zenodo, https://doi.org/10.5281/zenodo.5571936, 2021.

Zanaga, D., Van De Kerchove, R., Daems, D., De Keersmaecker, W., Brockmann, C., Kirches, G., Wevers, J., Cartus, O., Santoro, M., Fritz, S., Lesiv, M., Herold, M., Tsendbazar, N., Xu, P., Ramoino, F., and Arino, O.: ESA WorldCover 10 m 2021 v200, Zenodo, https://doi.org/10.5281/zenodo.7254221, 2022.